Nanotechnology in medical applications: Risk management issues for emerging technologies.

R.E. Geertsma[1], B. Roszek[1], S.L. Hoekstra-van den Bosch[2], W.H. de Jong[3]

[1]Centre for Biological Medicines and Medical Technology, National Institute for Public Health and the Environment (RIVM), PO Box 1, NL-3720 BA Bilthoven, The Netherlands [2]Ministry of Health, Welfare and Sport, The Hague, The Netherlands, [3]Laboratory for Toxicology, Pathology and Genetics, RIVM

Nanotechnology is an enabling technology which in some way will have an impact on many of the currently emerging medical technologies. The potential impact of novel nanotechnology applications on disease diagnosis, therapy, and prevention is foreseen to change health care in a fundamental way. In particular, relevant nanomedical applications are reported in surgery, cancer diagnosis and therapy, biodetection of disease markers, molecular imaging, implant technology, tissue engineering, and devices for drug, protein, and gene delivery. An increasing number of products are currently under clinical investigation and some products are already commercially available [1]. While product development is progressing rapidly, sufficient knowledge on the associated toxicological risks is still lacking. Reducing the size of structures to nanolevel may result in distinctly different properties. For medical applications utilising free nanoparticles or nanostructures, the specific toxicological properties have to be investigated [2]. Also for the toxicokinetic properties (absorption, distribution, metabolism, excretion) of nanoparticles there is an important knowledge gap. It is insufficient to rely on knowledge of the classical toxicity testing of bulk chemical(s) and materials when the risks of nanoparticles and/or nanostructures have to be assessed. RIVM has published two reports [1-2] on nanotechnology in medical applications addressing these topics and is currently carrying out further research. A study in rats has shown that gold nanoparticles exhibit an organ distribution after intravenous administration which is dependent on particle size [3]. The New & Emerging Technologies in Medical Devices Working Group of the European Commission has discussed risk management issues for medical devices utilising nanotechnology and is considering the adequacy of the existing medical devices regulatory regime to deal with these issues. The conclusion of the working group is that, in general, the medical devices directives are adequate to deal with medical devices manufactured utilising nanotechnology. However, because of the specific aspects of nanotechnology and the existing knowledge gaps, recommendations have been formulated for implementation aspects of the directives and for regulatory guidance. A specific recommendation is the introduction of a new classification rule for products utilising free nanoparticles, to the effect that “All devices incorporating or consisting of particles, components or devices at the nanoscale are in the highest risk Class III unless they are encapsulated or bound in such a manner that they cannot be released to the patient's organs, tissues, cells or molecules”. Furthermore, development of regulatory guidance, new mandates for standardization and consideration of the risks of disposal into the environment are recommended. A key starting point for any discussions regarding risks and regulations for medical technology based on nanotechnology is that there should always be a balance: patient safety should be protected without hampering innovation.

REFERENCES: [1] B. Roszek, W.H. de Jong, R.E. Geertsma (2005). Nanotechnology for medical applications: state-of-the-art in materials and devices. RIVM-report 265001001. RIVM, National Institute for Public Health and the Environment, Bilthoven, The Netherlands. http://www.rivm.nl/bibliotheek/rapporten/265001001.html. [2] W.H. de Jong, B. Roszek, R.E. Geertsma (2005). Nanotechnology in medical applications: Possible risks for human health. RIVM report 265001001. RIVM, National Institute for Public Health and the Environment, Bilthoven, The Netherlands. http://www.rivm.nl/bibliotheek/rapporten/265001002.html. [3] W.H. de Jong, W.I. Hagens, P. Krystek, et al. (2007). Particle size dependent organ distribution of gold nanoparticles after intravenous administration - a quantitative approach. *In preparation.*

ACKNOWLEDGEMENTS: The European Commission Working Group on New & Emerging Technologies in Medical Devices for constructive discussions.

Chitosan-Based Nanoparticles for Medical Applications – Stability in Physiological Environments

P. Käuper[1], N. Rossi[1], C. Laue[1], F. Schmitt[2], L. Lagopoulos[2], L. Juillerat[2], C. Wandrey[3]

[1] Medipol SA, Lausanne, Switzerland. [2] CHUV Lausanne, Switzerland.
[3] EPF Lausanne, Lausanne, Switzerland.

INTRODUCTION: Polyelectrolyte complex formation between the polycation chitosan and polyanions is an attractive, mild procedure to obtain nanoparticles potentially suited for medical applications; such as vectors for genetic materials [1]. A specific interest in employing chitosan as material in nanoparticle formulations foreseen for medical applications is its outstanding biocompatibility compared to other polycations [2,3]. Nanoparticles should be compatible with different *in vivo* environments. Literature-described chitosan-based systems showed limited stability [4]. Such compatibility aspects of chitosan-based nanoparticles will be highlighted in this presentation.

METHODS: Active components, to be retained by ionic interactions in nanoparticles, can be entrapped by addition during the nanoparticle formation process, or by subsequent loading. These production processes can be executed at conditions favouring different parameters such as stability of the nanoparticle dispersion or the active component stability. A successful design of drug-loaded nanoparticles takes further into account the requirements of conditioning such as sterilization, long-term storage and short-term *pre vivo* stability. Furthermore, the functioning *in vivo* should be tested (e.g. compatibility with condition at side of injection, targeting). In the herein presented work chitosan-based nanoparticles were tested with respect to their stability, i.e. resistance towards aggregation phenomena, at physiological salt concentrations, physiological pH, and injections into diluted and undiluted serum, serum protein solutions or synovial fluids. Finally, the applicability of sterilization and drying processes was evaluated.

RESULTS: Chitosan-based nanoparticles, loaded or unloaded and of positive zeta potential, showed instability towards physiological salt solutions and physiological pH values. Aggregation phenomena were found time and temperature dependent. Addition of uncharged molecules, such as sugars as cryoprotectives, was tolerated and led to formulations which can be freeze dried and redispersed. Time and concentration dependent aggregation phenomena were found if the nanoparticles were challenged with serum proteins or synovial liquids. Tailoring the particle surface towards a specific application seems necessary to render the particles compatible with physiological environments and to reach specific targets *in vivo*.

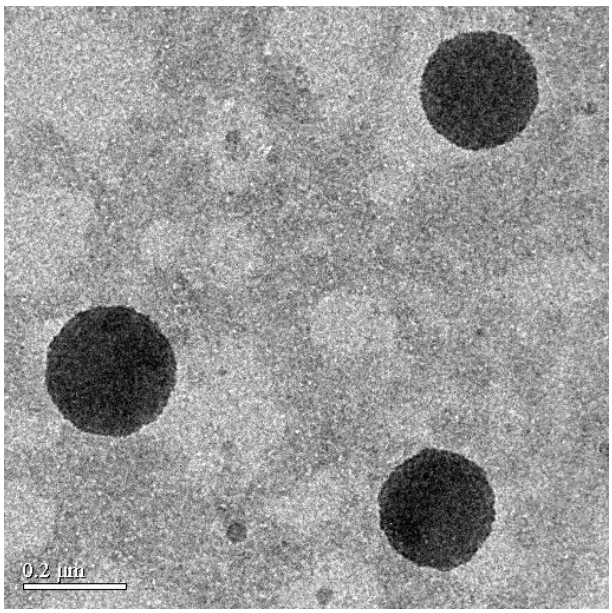

Fig. 1: Electron microscopic picture of chitosan-polyanion nanoparticles.

DISCUSSION & CONCLUSIONS: The stability of chitosan-based nanoparticles can be improved. A prerequisite is that the complex formed between the protonated amino function of chitosan and a polyanion's anionic function withstands physiological pH conditions. This could be confirmed by our studies. Tailoring the surface is the key to reduce the interaction with negatively charged surfaces (e.g. cell membranes) and molecules (e.g. negatively charged proteins) *in vivo* conditions.

REFERENCES: [1] H. Katas et al. (2006) *J Contr Rel* **115**:216-225. [2] H. Lv et al. (2006) *J Contr Rel* **114**:100-109. [3] S. Agnihotri et al. (2004) *J Contr Rel* **100**:5-28. [4]Q. Gan et al. (2005) *Coll Surf B: Biointerf* **44**:65-73.

ACKNOWLEDGEMENTS: The authors wish to thank the CTI for the support granted to the CTI project no 7985.2 LSPP-LS.

Comparison of amorphous TCP nanoparticles to micron-sized α-TCP as starting materials for calcium phosphate cements

T.J. Brunner[1], M. Bohner[2], C. Dora[3], C. Gerber[3], W.J. Stark[1]

[1] Institute for Chemical and Bioengineering, Department of Chemistry and Applied Biosciences, ETH Zurich, CH-8093 Zurich, Switzerland. [2] Dr. h.c. Robert Mathys Foundation, Bischmattstr. 12, CH-2544 Bettlach, Switzerland. [3] Department of Orthopaedic Surgery, University of Zurich, Balgrist, Forchstrasse 340, CH-8008 Zurich, Switzerland.

INTRODUCTION: Bone repair and regeneration of defects arising from trauma, tumor or bone diseases display a serious clinical problem in orthopedic surgery. Injectable and resorbable calcium phosphate compounds (CaP) have gained great importance due to their biocompatibility, bioactivity and osteoconductivity and the possibility of minimal invasive surgery. Apatitic calcium phosphate cements (CPC) cure by the reaction of a metastable CaP (e.g. α-TCP). This work describes the use of amorphous TCP, a high-temperature, metastable TCP in the form of nanoparticles for application in apatitic CPCs.

METHODS: The XRD-amorphous TCP (ATCP) nanoparticles were synthesized by flame spray synthesis [1] whereas α-TCP was prepared by solid state chemistry [2]. Reactivity of pure and mixtures of ATCP and α-TCP were tested using isothermal calorimetry. Further analyses included XRD, specific surface area and electron microscopy before and after setting as well as compressive strength and setting time.

RESULTS: Isothermal calorimetry results showed that the ATCP material reacted considerably faster when hydrated with Na_2HPO_4 than the micron-sized α-TCP. The energy release for the ATCP cement was short and intensive (finished after 40 min) whereas the α-TCP reacted for several hours to days. The specific surface area of the set cements, which is very important for the interaction with the implantation site, followed the addition of amorphous material and reached values of up to 160 m^2/g for pure ATCP [3]. The high surface areas are in agreement with the nanostructure of the newly formed apatite crystals shown in Fig. 1.

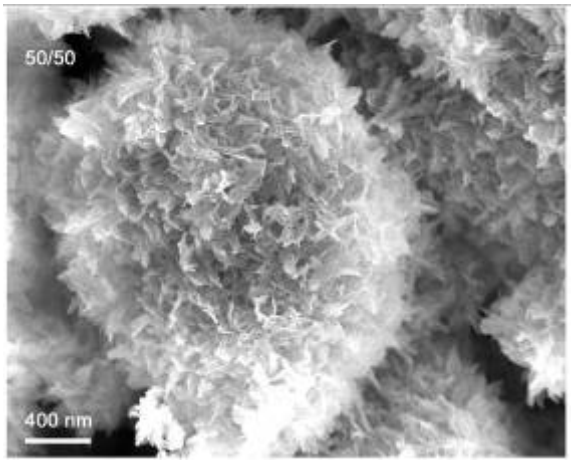

Fig. 1: SEM image of a 50/50 (w/w) mixture of ATCP/α-TCP after setting showing the formation of nanocrystalline apatite.

CONCLUSIONS:
The results clarified the importance of both particle size and phase of TCP on the reaction kinetics of apatitic CPCs. The described aerosol-derived ATCP nanoparticles are an interesting and promising starting material for the use in apatitic cements.

REFERENCES: [1] Loher S, Stark WJ, Maciejewski M et al., *Chem Mater* **2005**;17(1):36-42. [2] Camire CL, Gbureck U, Hirsiger W et al., *Biomaterials* **2005**;26(16):2787-2794. [3] Brunner TJ, Bohner M, Dora C, Gerber C, Stark WJ, *J Biomed Mater Res*, in review.

ACKNOWLEDGEMENTS: Financial support by the Gebert Rüf Foundation and the ResOrtho Foundation is kindly acknowledged.

Isothermal Microcalorimetry of Growth of an Oral Streptococcus Species and its Adhesion to Glass Beads

I. Hauser-Gerspach[1], P. Scandiucci de Freitas[2], AU. Daniels[2], J. Meyer[1]

[1] *Institute of Preventive Dentistry and Oral Microbiology, Dental School* [2] *Laboratory for Orthopedic Biomechanics, University of Basel, Switzerland.*

INTRODUCTION: Bacterial adhesion is the first step in the development of the oral biofilm, called dental plaque. Microorganisms adhere to the saliva-coated human tooth surfaces or dental materials within minutes after tooth cleaning. Plaque is the cause of dental caries, periodontal diseases and peri-implantitis. The range of microorganisms their physiological status and interactions in plaque formation are complex. Previously-published investigations of dental plaque, including bacterial adhesion, employ various in vivo and in vitro models and use microscopic methods to assess surface interactions [1]. Microcalorimetry offers another direct approach, potentially allowing one to measure the energetics of the adhesion process.

METHODS: *Streptococcus sanguinis*, one of the first colonizers, was used as the model organism. TAM III™ thermostats, equipped with microcalorimeters (Thermometric AB, Järfälla, Sweden) were used for isothermal microcalorimetric (IMC) measurements of heat production (µJ/sec=µW) of bacterial growth in Schaedler broth as a function of time expressed by power-time (p-t) curves. To detect heat flow during adhesion of bacteria to glass beads, replication and nearly all metabolic activity were minimized by using stationary *S. sanguinis* suspended in a liquid with either, no nutrition source, PBS, or a very limited one, human saliva.

RESULTS: Replication of an initial concentration of $5x10^6$ *S. sanguinis* cells/ml in Schaedler broth produced a characteristic p-t curve with a maximum of 500 µW when reaching 10^9 cells/ml. A lower concentration of the start inoculum ($5x10^5$ cells/ml) led to almost identical p-t curve demonstrating the high reproducibility of the IMC method. In contrast, 10^9 cells/ml of non-replicating *S. sanguinis* cells, suspended in PBS produced only ~30 µW maximum. But the amount of heat increased with available glass surface area (Table1), indicating that a portion of the heat of adhesion was measured. Stationary *S. sanguinis* cells, suspended in human saliva to mimic conditions of the mouth, resulted in slightly higher energy release. These differences could be related to interactions of proteins or other large molecules in the saliva with the bacteria or residual metabolism rather than to bacteria alone.

Table1. Mean cumulative heat production (µJ) during 1 h adhesion of S. sanguinis (n=10)

Liquid	Glass ampoule	Ampoule +0.3g glass	Ampoule +3.0g glass
PBS	74,800	79,500	91,000
saliva	84,400	94,600	107,000

DISCUSSION & CONCLUSIONS: This study shows that microcalorimetric evaluation of initial bacterial adhesion is indeed possible and may become a rapid and reproducible screening method to study adhesion of different bacteria to different dental materials or modified surfaces. It could be useful to identify bacterial surface molecules involved in adhesion by comparing suitable bacterial mutant strains. It could also be developed into a convenient screening method to compare different dental materials or materials subjected to different surface treatments with the aim of reducing adhesion. Further, it could provide valuable information on interfering substances to be applied in oral prophylaxis.
Detailed results will be published [2].

REFERENCES: [1]I. Hauser-Gerspach, E.M. Kulik, R. Weiger, et al. (2007) *Dent Mater J* 26 (3). [2]I. Hauser-Gerspach, P. Scandiucci de Freitas, AU. Daniels, et al. (2007) *J Biomed Mater Res B Appl Biomater* submitted.

ACKNOWLEDGEMENTS: Support from the following sources is gratefully acknowledged: SSO-Fonds für zahnärztliche Forschung (grant No. 224); Hardy u. Otto Frey-Zünd Foundation: LOB, general long-term support; Robert Mathys Foundation: LOB, 2004 Projekt P04E106 (IMC equipment grant); Velux Foundation: LOB, 2006 Research Grant 301 (IMC equipment, supplies and personnel support for IMC studies of microorganisms); Straumann AG, Basel.

Structural Investigation of Composite Biomaterials for Hyperthermia

V. Simon[1], H. Mocuta[1,2], D. Eniu[3], D. Trandafir[1,2], S. Simon[1,2]
[1] *Babes-Bolyai University, Faculty of Physics, Cluj-Napoca, Romania.* [2] *Institute for Interdisciplinary Experimental Research of Babes-Bolyai University, Cluj-Napoca, Romania.*
[3] *University of Medicine and Pharmacy, Faculty of Pharmacy, Cluj-Napoca, Romania.*

INTRODUCTION: Localized hyperthermia is a therapeutic procedure used to raise the temperature of a region of the body affected by cancer. The treatment is based on a direct cell-killing effect at temperatures above 43°C. Our studies are focused on iron containing aluminosilicate composite materials able to develop nanocrystalline magnetic phases as heating media for cancer treatment.

In nanostructured composite materials, beside composition the knowledge of the structure is a key requirement for understanding materials properties. Since the X-ray wavelengths are in the same order as the sizes of nanostructures, we used X-ray diffraction to investigate the composite architecture.

METHODS: Samples belonging to $xFe_2O_3(80\text{-}x)SiO_2{\cdot}20Al_2O_3$ system ($5 \leq x \leq 20$ mol %) were prepared by the sol-gel method starting from silicic acid as source of silica, iron and alumina nitrates. The sludges were stirred at room temperature for 3 hours and the precipitates were filtered. Reddish coloured solid sample were obtained after drying at 110°C. The dried samples were subjected to heat treatments carried out at 500°C for 1 hr and at 1200°C for 24 hrs.

The structure of the thermal treated samples was investigated by XRD with a Shimatsu diffractometer using CuK_α radiation. The average crystallite size was estimated by using the Scherrer equation:

$$D = \frac{k\lambda}{\beta \cos\theta}$$

where D is the crystallite size, λ is the X-ray wavelength, k is the shape factor equal to 0.9, θ is the diffraction angle of selected line and $\beta = \sqrt{B^2 - b^2}$, where B is the full width at half maximum intensity and b the resolution parameter of the diffractometer.

Electron paramagnetic resonance (EPR) measurements were carried out in these samples on ADANI PS 8400 system EPR spectrometer, in the magnetic field range of 700-4700 Gauss, in the X-band, at room temperature.

RESULTS & DISCUSSION: The heat treatment applied at 500°C does not lead to crystalline phase development, but that applied at 1200°C (Fig. 1) mainly determines the grows of hematite nanocrystals. Selection of a reducing atmosphere will be able to produce a finely dispersed magnetite the samples [1].

The size of hematite crystals determined using Scherrer formula is about 8.7 nm. DRX data also evidence aluminosilicate crystals of mullite ($Al_6Si_2O_{13}$) type [2] that confer to samples a high structural stability.

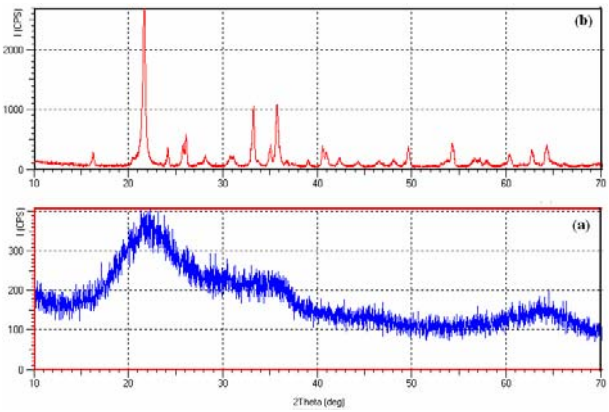

Fig. 1: XRD patterns of samples with 20 mol% Fe_2O_3 heat treated at 500°C (a) and 1200°C (b).

The EPR results obtained for as prepared samples are specific to disordered oxide systems with high Fe_2O_3 content. The resonance line at $g \approx 2.0$ is shifted to lower values of the magnetic field when the iron oxide content increases. The spectra of the heat treated samples contain an additional narrow line at $g \approx 4.3$ arising from Fe^{3+} ions disposed in the crystalline phases well developed during the applied heat treatment.

CONCLUSIONS: The non-crystalline state of iron containing aluminosilicate samples obtained by sol-gel route is transformed by heat treatment applied at 1200°C in a structural stable composite material with hematite nanocrystals and $Al_6Si_2O_{13}$ crystals.

REFERENCES: [1] K.A. Gross, R. Jackson, J.D. Cashion, et al (2002) *Eur Cell Mater* **3** Suppl.**2**:114-17. [2] P. Hou, S.N. Basu,V.K. Sarin (1999) *J Mater Res*, 14:2952-58.

ACKNOWLEDGEMENTS: The present work was supported by the scientific research project CEEX 100/2006 (MATNANTECH) of the Romanian Excellence Research Program.

Fabrication and study of mechanical properties of Poly-L-lactic / nanoHydroxyapatite dense composites for bone tissue engineering

S.Arostegui, S.Gay, J.Lemaître

Laboratory of Powder Technology, EPFL, CH-1015 Lausanne, Switzerland.

INTRODUCTION: The number of high skeletal defects found in a wide variety of clinical situations keeps increasing. Current clinical therapies do not satisfy the existent needs; there is a real demand for alternative bone substitutes and improved wound healing therapies. Nanocomposite materials mimicking the microstructure of bone would probably have a good chance to achieve expected properties for bone substitutes. Poly-L-Lactic (PLLA) matrix dense composites reinforced with nanosized hydroxyapatite particles (nHA) with three particle concentrations (0, 25 and 50%wt HA) were prepared and characterized in order to estimate the intrinsic mechanical properties of the material. The effect of an annealing post-treatment was also analysed.

METHODS: Solvent casting-hot pressing method was used to prepare test samples. Commercial hydroxyapatite was deagglomerated by attrition-milling. Incorporation of nHA particles into the polymer was facilitated by a solvent exchange process, substituting the initial aqueous medium by chloroform. After chloroform evaporation at room temperature, dense cylindrical composite test samples were made by hot-pressing at 190°C (relative density > 97%). Mechanical properties were estimated by uni-axial compression and Brazilian tests (indirect tensile test).

Thermal, microstructural and physical properties of the composites were also measured (DSC, EDX, FTIR, TEM, X-ray diffraction, contact angles), but will be presented in detail elsewhere.

RESULTS: The mechanical properties of the samples changed markedly depending on their nHA content. The applied annealing treatment had no effect on the properties, and did not modify the cristallinity of the polymer matrix. Ultimate stresses obtained in both tests were analysed by the Mohr's circle approach [1], in order to estimate the intrinsic characteristic properties of the composites (*Table 1*). Neat PLLA is not shown because it could not be represented by the Mohr's approach due to its excessive ductility.

Young's compression modulus was calculated from the slope of the linear region of the stress-strain curve by least-square regression. *Figure 1* presents the Young's compression modulus in function of nHA content. Young's modulus increases linearly with ceramic content.

Table 1. Intrinsic characteristic normal strength (σ_0) and shear strength (τ_0) of composites compared to cortical bone.

	σ_0 [MPa]	τ_0 [MPa]
Cortical bone [2]	145-235	50-80
PLLA/25%nHA	57	34
PLLA/50%nHA	80	40

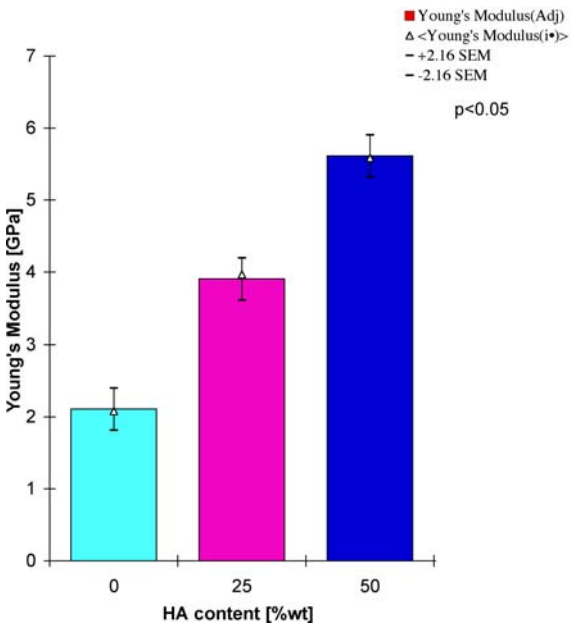

Figure 1: Young's compression modulus vs *nHA content of nHA/PLLA dense composites.*

DISCUSSION & CONCLUSIONS: Dense PLLA/nHA composites containing up to 50%wt nHA were successfully prepared by solvent casting/hot pressing method.

Mechanical performance of PLLA/nHA composite was enhanced by increasing nHA content, leading to mechanical properties commensurate to those of human cortical bone.

REFERENCES: [1] C. Pittet, J. Lemaître (2000) *J Biomed Mater Res* **53**:769-780. [2]A. Ravaglioli and A. Krajewski, (2003) *Bioceramics. Materials Properties Applications*, Chapman & Hall.

ACKNOWLEDGEMENTS: This work is part of the NANOBIOCOM project supported by the 6th Framework European R&D Program (Project n° NMP3-CT-2005-516943).

In Vitro Effect of Surface Polishing for Reducing Bony-overgrowth.

J.S.Hayes [1,2], C.W.Archer [2], R.G.Richards[1]

[1]*AO Research Institute, Clavadelerstrasse 8, Davos CH7270, Switzerland.*
[2]*CTBL, Cardiff School of Biosciences, Cardiff Univeristy, CF10 3US, Wales, UK.*

Introduction: The necessity of implant removal, chiefly within the paediatric population is widely accepted on the grounds of avoiding difficulties such as infection, adverse tissue reaction & the hindrance of bone remodeling[1]. However problems associated with device removal are commonplace & can occur mainly as a result of the complete bony-integration of a device. In clinical terms this is highly undesirable, causing increased operative time & blood loss as well as negatively influencing the healing process. Therefore, we investigated the potential of surface polishing of titanium & its alloys to reduce over-integration of a device from a cellular level, since the surface micro-topography of a material has been shown extensively to be a principle determinant of tissue integration[2].

Methods: Commercially pure titanium (cpTi), Titanium6%Niobium7%Aluminium (TAN), Titanium15%Molybdenum (Ti15Mo) & Stainless steel (Ss, negative control) were studied. Micro-rough standard surfaces of the cpTi (TS), TAN (NS) and Ti15Mo (MS) were included as positive controls for osseointegration. The latter were also electro- (TE, NE, ME)& paste (TP, NP, MP) polished to produce experimental smooth surfaces, determined by AFM, non-contact profilometry, XPS & SEM. Response of 6 day old primary rat calvaria (RC) cells to the surfaces was investigated. Osteocalcin (OC) gene expression,^{3}H-thymidine incorporation (^{3}HTdr);10μCi/ml) & DNA content (Hoechst 33258) were studied over 21 days.

Results/Discussion: Polishing of the substrates reduced surface micro-roughness dramatically compared to positive controls while XPS showed that polishing followed by anodisation did not affect the final surface chemical properties. Using SYBR green qPCR technology for relative OC gene expression (Fig.1) we showed a significant decrease (ANOVA $p<0.05$) for both polished variants regardless of material type. DNA quantification (Fig.2) revealed that while paste polished surfaces maintained DNA levels in line with that of the negative control (i.e. increased over positive controls) electro-polished samples had a significant augmentation. An inverse relationship between mineralization & DNA content was noted. ^{3}HTdr incorporation results show individual proliferative outcomes for all samples with a general peak being observed at 14 days. Interestingly, NP had stunted proliferation compared to other samples. Ongoing viability and morphological analysis will aid in elucidating this observation. Collectively this data indicates that while a mature osteoblast phenotype is observed on standard micro-rough surfaces, cells on polished samples are unable to maintain this phenotype hence adopt a cell proliferative state.. Polishing essentially reduces the ability cells to form new bone at the bone interface.

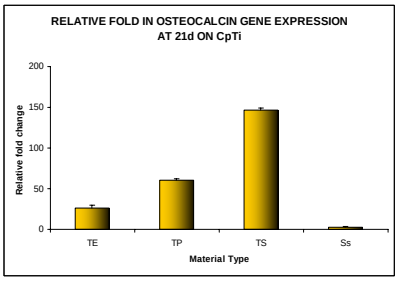

Figure1. OC gene expression RC cells on cpTi at 21 days. Both polished variants have significantly ($p<0.05$) lower OC gene expression, for cpTi, TAN & Ti15Mo samples.

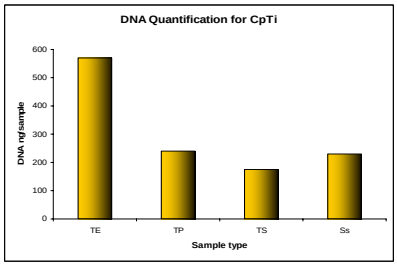

Figure 2. DNA content results for cpTi at 21 days.A similar trend is observed for TAN and Ti15Mo samples also. .

Conclusions: Surface polishing acts on a cell level to reduce osteoblast differentiation & subsequent mineralization. This will have application for devices destined for elective removal.

References: [1] Peterson.(2005) Metallic Implant removal in Children. J. Paediatric. Orthop. 25: 107-115. [2] Meredith et al., (2007) Is surface chemical composition important for orthopaedic implant materials? J Mater Sci. Med 18: 405-413.

Acknowledgments: Dr. I.M Khan, Cardiff University for qPCR discussion. Dr. V Frauchiger, RMS, Bettlach for XPS. Dr. D.M Devine, Athlone Institute of Technology for AFM imaging.

Fine-tuning of cochlear implant material-cell interactions by femtosecond laser microstructuring

G. Reuter[1], U. Reich[1], P.P. Müller[2], T. Stöver[1], E. Fadeeva[3], B. Chichkov[3], T. Lenarz[1]

[1] Department of Otolaryngology, Medical University of Hannover, Germany, [2]Helmholtz Centre for Infection Research, Braunschweig, Germany, [3]Laser Zentrum Hannover e.V., Germany

INTRODUCTION: Optimal electrical stimulation of neuronal cells requires a close position of the electrodes to the neuronal structure and low impedance of the electrode contacts. In case of the cochlear implant, the interaction to the cells of the connective tissue growth is important. After implantation of the CI electrode an increase of impedance can be observed, which may be affected by the growth of connective tissue around the electrode. In addition, the electrical stimulation signal becomes more unspecific. The aim of our research project is the physical modification of the electrode surface [1, 2, 3] to create an "unattractive" surface for tissue growth and to increase the electrical contact to the neuronal cells. This should work in different types of electrodes inserted into the midbrain, on the surface of a target region such as the brainstem, or in fluid-filled scalae such as the scala tympani in the inner ear.

METHODS: The cochlear implant electrode contains 22 platinum electrode contacts on a silicone carrier. The silicone carrier is manufactured by Cochlear Ltd, Sydney from two types of silicone (LSR 30, HCRP 50). For our studies we use silicone sheets (LSR 30) with rough and smooth surface, moulded silicone LSR 30 and rough silicone HCRP 50. As a model for the platinum contact material we used a micro-structured and platinum sputtered glass wafer. With the femtosecond laser technology geometric microstructures were produced on the surface of the materials with a width of 1-10 µm and a depth of appr. 1 µm. In case of the silicone sheets the micro structure was produced via laser ablation. For the moulded silicone the micro structured glass wafer was used as the mould. GFP-marked fibroblasts allow to observe cell morphology and cell growth in correlation with the structure geometry also on the non-transparent materials. Cell growth can be observed on one sample over a period of several days which makes this method particularly suitable for trials with only few samples [4].

RESULTS: Rapid progress of femtosecond laser systems and unique characteristics of ultrafast laser pulses open up new possibilities for high-precision contact-free material micromachining. Direct femtosecond laser ablation enables fabrication of high-quality structures in almost all solid materials with a resolution down to 100 nm.

The fibroblasts grow on the electrode materials. The cell growth rate on all kinds of silicone is significantly lower than on platinum. Polished silicone surface decreases cell growth on silicone. The laser structure further reduced the growth of fibroblasts. After 3 days of cell culture the number of cells on the microstructured platinum was significantly reduced. On all types of the silicones the effect of the microstructuring was also visible. On LSR 30 with smooth surface the reduction during the microstructure tends to be larger than on the rough surface and also larger then on the moulded silicone.

On platinum we observed a maximal effect of the microstructuring procession to the cell growth on a structure width of 4-7 µm but not as strong on smaller (1-4 µm) and larger (7-10 µm) grooves. An analog result was observed on silicone LSR 30 with a rough surface quality.

DISCUSSION & CONCLUSIONS: GFP-marked fibroblasts are a model for connective tissue cells. The microstructure affected fibroblast growth and guided neuronal cell growth. In further experiments structures of different sizes are to be tested on several electrode materials. The aim is to optimise the electrode interface, to reduce the connective tissue growth and to improve the electric contact to the neuronal target cells.

REFERENCES: [1] Den Braber, ET, Ruijter, JE, Ginsel, LA, von Recum, AF, Jansen, JA (1998) *J Biomed Mater Res*, **40**: 291-300. [2] Yoshinari, M, Matsuzaka, K, Inoue, T, Oda, Y, Shimono, M. (2003) *J Biomed Mater Res A* **65**: 359-68. [3] Rajnicek, AM, Britland, S, McCaig, CD, (1997) *J Cell Sci*, **110**: 2905-291. [4] Reich, U, Reuter, G, Müller, P, Stöver, T, Lubatschowski, H, Lenarz, T (2005), *Biomaterialien* **6**: 194

ACKNOWLEDGEMENTS: This project was supported by the German Research Foundation, Collaborative Research Centre 599: "Sustainable Bioresorbable and Permanent Implants of Metallic and Ceramic Materials"

Selection of synthetic extracellular matrices for cardiac muscle tissue engineering.

G Fortunato[1], D Keller[2], D Balazs[1], E Körner[1], T Humbert[1], H Tevaearai[2], MN Giraud[2]
[1]*EMPA, Saint Gallen, Switzerland.* [2] *Swiss cardiovascular Center, Bern, Switzerland.*

INTRODUCTION: Progress in tissue engineering is conditioned by the creation of a suitable environment in which cells can grow and organize themselves in a functional way. The development of biocompatible materials that would mimics the extracellular matrices hold technical and biological importance. We addressed the role of nano- and micron-sized fiber structures in muscle cell adhesion, growth, guidance and differentiation.

METHODS: The nano- and micron-sized non-wovens were prepared by an electrospinning procedure. Therefore, the biocompatible polymers polycaprolactone (PCL), poly(l-lactic acid) PLLA , polyethylene carbonate (PEC) as well as collagen were dissolved in appropriate solvents and spun by applying a high voltage on a needle tip. Partial parallelisation of the nanofibers was obtained by using electrostatic lens systems and a fast rotating drum. Selected fiber patches were coated with a nitrogen-functionalized amorphous hydrocarbon coating (a-C:H:N), by performing RF plasma deposition using a gaseous mixture of ammonia and ethylene.

Myoblasts cell lines (C2C12) as well as rat skeletal muscles primary cell culture were seeded on the surface of biomaterials and cultured for up to 2 weeks in growth and differentiation media. We used MTT staining to assess cell adhesion and viability after 2 days, Hematoxylin-Eosin staining and immunostaining to assess cell morphology, alignment and differentiation.

RESULTS: The chemical and instrumental parameters used for the elelctrospinning procedure revealed a deep influence with respect to the PCL fiber diameters. Fibers with diameters from 100 nm to 2500 nm could be obtained. Main influencing parameters were the composition of the solvents used and the applied voltage.
Cell adhesion was dependant on the incubation of the materials with the adhesive protein, laminin, and was inversely proportional of the biomaterials wetttability (Spearman correlation coefficient r=-0.55, ns). Guidance of the cell seeded on parallel nanofibers was observed at low cell density. Growth and differentiation of the cells was reduced when compared to standard cell culture in plastic dishes. Interestingly, surface coating by plasma treatment of the biomaterials with the a-C:H:N provided an optimal cell adhesion that was increased by at least 20% with respect to non-coated patches. The a-C:H:N coating on PCL yielded a reduction in water contact angle from 132° to 14°. Cell presented a specific differentiation response to C:H:N coating with elongated and parallel myotubes.

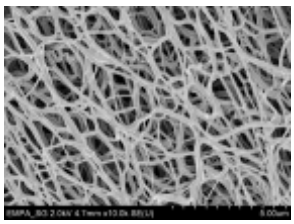

Fig. 1. Polycaprolactone (PCL) nanofibers produced by an electrospinning procedure (fiber diameter ca. 100 nm)

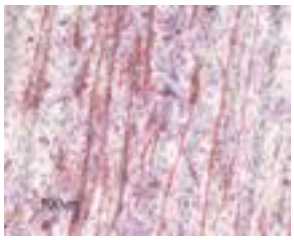

Fig.2. Aligned and elongated myotubes obtained from myoblast primary cell culture on a-C:H:N coated PCL (desmin immunostaining)

DISCUSSION & CONCLUSIONS: Our results provide evidence that optimization of bioartificial tissue construct using nanofibers is challenged by biomaterials properties such as wettability, alignment of the fibers and coating. In addition In addition parameters such as elasticity and porosity have to be considered for cell differentiation and the construction of a 3 dimensional bioartificial tissue. Furthermore, functional biografts would ideally contract under electrical stimulation and sustain the high mechanical stress represented by the permanent cardiac muscle contraction/relaxation cycles. Replacement of the cardiac native muscle requires the engineering of a complex muscle tissue that would largely benefit from the electrospin and plasma coating technologies.

SuperParamagnetic Iron Oxide Nanoparticles: a multifunctional tool in biomedical applications

F.Cengelli[1], F. Tschudi-Monnet[2], D. Maysinger[3], X. Montet[4], A. Montoro[1], A. Ferrari[5], A. Petri-Fink[5], H. Hofmann[5], L. Juillerat-Jeanneret[1]

[1]University Institute of Pathology, University of Lausanne, Lausanne, Switzerland. [2]Institute of Physiology, University of Lausanne, Lausanne, Switzerland. [3]Department of Pharmacology, McGill University, Montreal, Canada. [4]Department of Cell Physiology and Metabolism and Medical Radiology, University of Geneva, Geneva, Switzerland. [5]EPF Lausanne, Lausanne, Switzerland.

INTRODUCTION: We have previously developed SuperParamagnetic Iron Oxide Nanoparticles (SPIONs) with a core size of 9-10 nm diameter and a coating made of polyvinyl alcohols (PVA) [1]. Our objectives are to evaluate their biocompatibility, their potential for uptake by cells and their cellular localization in various types of cells in culture and in organs in animal models.

METHODS: To evaluate cell uptake we used either 2-dimensional and 3-dimensional cell culture models, tumor cell spheroids and brain cell aggregates. In animal models, SPIONs were injected i.v. in normal mice, and organs were examined for their SPIONs content. In order to evaluate the cell and tissue uptake of these SPIONs we combined detection of their fluorescent coating, of the iron oxide core using confocal microscopy, prussian blue detection of iron and transmission electron microscopy. In order to determine their biocompatibility we evaluated cell survival by evaluating mitochondrial activity and DNA synthesis.

RESULTS & DISCUSSION: We showed that in 2-dimensional cell cultures the presence of amino groups on the SPIONs coating was mandatory for cell uptake, and this uptake did not modify cell proliferation. SPIONs uptake by cells was increased in the presence of an external magnetic field. The results demonstrated that the polymer coating and the iron oxide core of SPIONs can be internalized by cells *in vitro* (Fig. 1). In various tridimensional cell culture models SPIONs were found associated with cells, being able to invade tumor spheroids but not differentiated brain aggregates [2]. *In vivo* SPIONs were found associated with cells in the spleen and the liver but not the brain and kidneys.

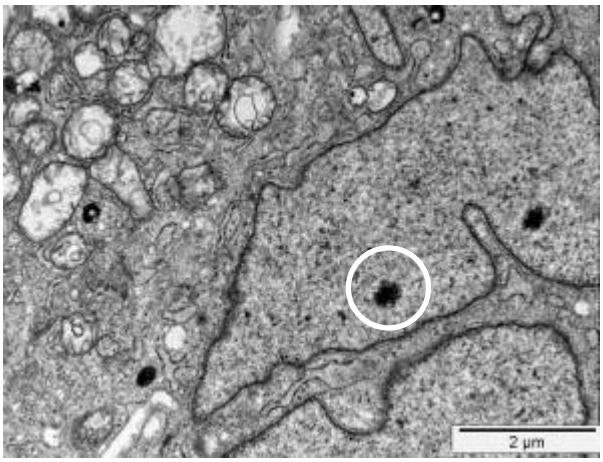

Fig. 1: Transmission electron microscopy showing aminoPVA-coated-SPIONs uptake in the nucleus of human melanoma cells, after 4h of exposure.

CONCLUSIONS: These approaches gave a proof of concept of the feasibility of using such SPIONs in biological systems, and their potential to be selectively taken up by living cells.

REFERENCES: [1] A. Petri-Fink, M. Chastellain, L. Juillerat-Jeanneret, et al (2005) *Biomaterials* **26**:2685-2694. [2] F. Cengelli, D. Maysinger, F. Tschudi-Monnet, et al (2006) *JPET* **318**:108-116.

ACKNOWLEDGMENTS: This work was supported by the Swiss National Scientific Research Foundation (Grant 3152A0-105705).

Effect of a serum free medium containing TGF-β_3 on osteocyte viability of cultured human cancellous bone explants

K. Jähn, M.J. Stoddart, P.I. Furlong, D.B.Jones[a], C.W. Archer[b], R.G. Richards
AO Research Institute, Davos, Switzerland; [a] Dept. of Orthopaedics & Biomechanics, Marburg University ,Germany [b]Cardiff School of Biosciences, Cardiff University, Cardiff CF10 3US, Wales.

INTRODUCTION: The replacement of Foetal calf serum (FCS) as a growth factor and hormone supplement in culture media would have major advantages in cell or organ culture. The factor concentrations within FCS are inconsistent and vary from batch to batch. This can cause unintended effects on cultured cell populations. Furthermore, the protein level in media with added FCS could cause problems, if investigation of secreted factors at low concentrations is intended. However, if using a serum free medium, problems arise in maintaining cell viability, which can be achieved by adding suitable factors. The aim of this study was to investigate the effect on osteocyte viability of a serum free medium containing 15 ng/ml TGF-β_3 during *ex vivo* culture of human cancellous bone explants.

METHODS: Human femoral heads (Ethic Commission Graubünden 18/02) from hip transplant patients were excised and cut into 7 mm thick sections with the use of an Exakt 300 band saw. Cores 9.5 mm in diameter were bored from the sections with Synthes drill bit (Ref: 387.661, Synthes, Bettlach, Switzerland) and cut parallel to 5 mm with a Leica annular saw. After insertion inside the culture chambers, cores were perfused with either DMEM + 10% FCS or DMEM serum free + 15 ng/ml TGF-β_3 (ITS and lipids supplemented). A daily load was applied with a complete jump wave form for 5 min (300 cycles, 1 Hz, 4,000 µstrain) using a Zetos bioreactor [1, 2]. After a culture period of 14days cores were harvested and cut to 250 µm sections down to the centre with a Leica annular saw. Surface and centre sections were assayed with LDH viability staining [3]. The sections were fixed in 4% buffered formalin and visualised using fluorescence and light microscopy (Axioplan).

RESULTS: Using the natural autofluorescence of the bone matrix, osteocyte viability of LDH stained sections was analyzed at 515-565 nm emission filter. Dark stained, viable osteocytes will efficiently block the autofluorescence, and viability quantification can be accomplished. In every case of performed three experiments, the use of DMEM serum free + 15 ng/ml TGF-β_3 (Fig.1B) showed similar or enhanced maintenance of osteocyte viability in core centres compared to the use of DMEM + 10% FCS (Fig.1A).

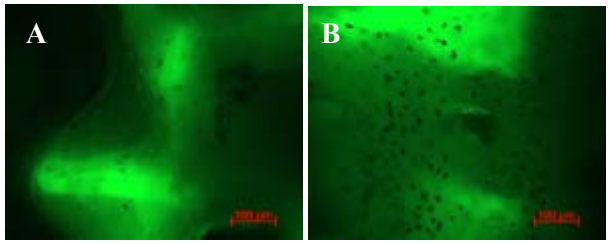

Fig. 1: Representative fluorescence pictures of LDH stained centre sections from human cancellous bone cores after 14 d culture.
***A:** Cultured in DMEM + 10 % FCS;*
***B:** Cultured in DMEM serum free + 15 ng/ml TGF-β_3.*

An additional effect using serum free medium was a reduction in the number of surface fibrous cells seen on cores cultured in serum containing medium. Fibroblast-like cells were found on 68% of cores cultured within serum containing medium. On the contrary 61% of the cores cultured in serum free medium did not show the fibrous tissue.

DISCUSSION & CONCLUSIONS: DMEM serum free with added 15 ng/ml TGF-β_3 seems suitable to replace the serum containing DMEM during culture of human cancellous bone cores, when looking at osteocyte viability and surface fibrous tissue formation. The reduction of the fibrous tissue will provide an even more defined culture environment, as the fibroblast-like cells would compete for nutrients, and are also likely to secrete unknown factors.

REFERENCES: [1]D.B. Jones *et al.* (2003). *Eur Cell Mater* **5**: 48-60; [2]C.M. Davies *et al.* (2006). *Eur Cell Mater* **11**: 57-75 ; [3]M.J. Stoddart *et al.* (2006). *Eur Cell Mater* **12**: 16-25

ACKNOWLEDGEMENTS: The authors would like to thank ESA MAP grant #AO99-122 for funding. Thanks to Dr. Thomas Perren (Davos Hospital), Dr. Heinz Bereiter (Chur Hospital) for supplying human tissue.

Optical Coherent Tomography Investigation on Apical Region of Dental Roots

C. Sinescu[1], A. Podoleanu[2], M. Negrutiu[1], M. Rominu[1]

[1] *University of Medicine and Pharmacy" Victor Babes" Timisoara, Romania*

[2] *University of Kent, United Kingdom*

INTRODUCTION: The purpose of this study is the investigation of the apical areas of the root using a noninvasive method. Optical coherence tomography is a well known technique for creating non-invasive, high resolution (< 20 μm) images of biological microstructure [1]. Dentists evaluate the oral health of a patient using three main techniques: visual/tactile examination, periodontal probing, and radiographic imaging. Probes are placed between the soft tissue and the tooth in order to assess periodontal conditions. The depth of the probe penetration (probable pocket depth) is measured. The location of the soft tissue attachment is estimated from a fixed reference point on the tooth. Periodontal probing can be painful for the patient and diagnostically imprecise. Probing errors result from variations in insertion force, inflammatory status of tissue, diameter of probe tips, and anatomical tooth contours. Radiographs reveal morphological characteristics of the teeth and of the alveolar bone that can not be identified in a visual examination. Although radiographs are highly sensitive in detecting regions of carious demineralization and alveolar bone loss, they have several limitations. Radiographs cannot distinguish active from inactive disease. Periodontal disease is not identified until significant bone loss has occurred. Since radiographs are bi-dimensional, it is impossible to precisely locate the position of a carious lesion or osseous defect. Radiography uses harmful ionizing radiation and provides no information on soft tissue state.

METHODS: The method is based on the optical coherence tomography (OCT) which can provide a lot of information about the apical zone of the dental root through a non-invasive procedure. For this analysis 34 extracted single root teeth were used. The apical area was scanned from apical to cervical. A schematic representation of OCT instrumentation is shown in Figure 1. It is based on a white light optic fibre Michelson interferometer. Mirror reflections and backscattered light from the sample are recombined at the coupler and propagated to the detector and light source. An interferometric signal is detected when the distance to the reference and sample arm reflections is matched within the source coherence length. A scanning retro-reflector varies in path length of the reference arm for each transverse location on the sample. The loss in the signal intensity caused by birefringence effects in the optical fiber is corrected using polarization paddles.

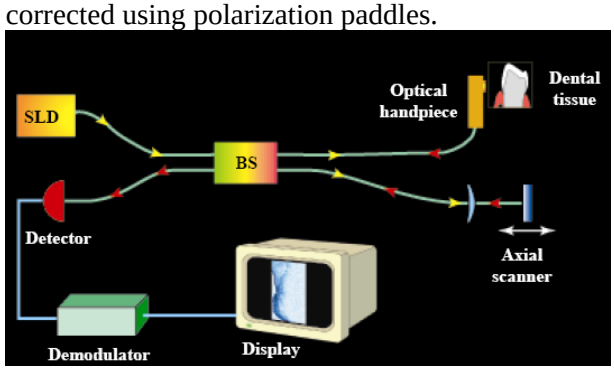

Fig.1. The scheme of dental OCT System.

RESULTS: The study provides images of many lateral canals that can be shown without sectioning the teeth. The accuracy of those images is very good for 2mm length of investigation. (Figure 2).

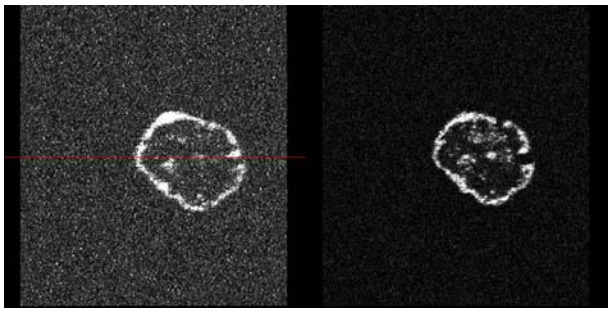

Fig. 2: OCT image of an apical zone of a single root tooth.

DISCUSSION & CONCLUSIONS: As a general conclusion, the optical coherence tomography can be used as a non-invasive method in the apical part of the teeth. This method can be used successfully in micro-leakage studies in order to offer accurate three-dimensional information.

REFERENCES: [1]R.G. Cucu, A.G. Podoleanu, J.A. Rogers, J. Pedro, R.B. Rosen (2006) *Optics Letters*, **31**,11:1684-1687.

Root Canal Tensions Investigated With Electric Tensional Stamps During the Rotative Instrumentation

C. Sinescu[1], M. Negrutiu[1], R. Negru[2], Z. Florita[1], N. Faur[2]

[1] *University of Medicine and Pharmacy "Victor Babes" Timisoara, Romania*

[2] *Polytechnics University of Timisoara, Romania*

INTRODUCTION: Root canal system preparation is one of the most important procedures during endodontic treatment. There has been a constant search for quicker, safer and more efficient methods for cleaning and shaping the root canals [1]. The purpose of this study is to describe a method for investigating the tensions in the prepared tooth, in order to be able to determine the maximum load that can lead to the fracture of the rotative instruments that were used in this procedure.

METHODS: Single rooted (n=10) and multiple rooted (n=10) teeth (extracted due to orthodontic reasons) were used in this experiment as samples. For each tooth the pulps were removed and prepared for root canal instrumentation. One set of root canal instrument was used (ProTaper, Maillefer) per each sample. Three electric tensional stamps were applied on each tooth (one in the cervical area, one in the middle area and one in the apical area).

Fig. 1. Precision sensors used in the study.

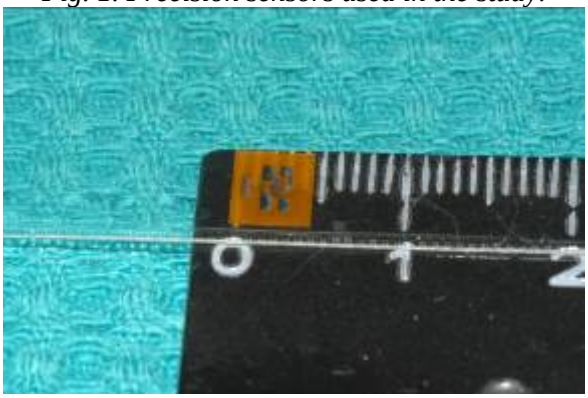

Fig. 2. Dimensions of the Precision sensors used in the study.

The method used in shaping the root canal was the crown-down procedure using rotative instruments (ProTaper). The root canal instrumentation was done at the following speeds: 400 rotation per minute (rpm), 300 rpm, 200 rpm and 100 rpm. One single rooted and one multiple rooted teeth were instrumented manually, in the step-back procedure. For each procedure mentioned above, the root canal preparation was done with and also without water irigation. The instrumentation of the roots was done, with all instruments from the ProTaper set to the F3 finishing file, except the situations where an instrument has broken during root canal shaping.

RESULTS: Tension changes varied significantly with the teeth, with the single or multiple root, the apical form of the root and the speed. Several fractures of the instruments inside the root canals were obtained and the variation of the tensions recorded on those teeth were analyzed. The maximum tensions were recorded in the apical and the middle area of the roots. Three ProTaper instruments were fractured in the multiple rooted teeth, in the apical area. The maximum tensions were obtained for the teeth in which the preparation was done without water irigation. For the apical regions, the fracture tensions recorded in the three cases reported above were also achieved in other teeth, in the same zone, without inducing the fracture. However, the tensions recorded were proportionally with the shaping speed.

DISCUSSION & CONCLUSIONS: The general conclusion of the study is that the root canals instrumentation represents a complex phenomenon, depending not only on the instrumentation speed and water cooling, but also on the elasticity modulus of each tooth area. This method allows the possibility to investigate the tensions that appear in the root during the root canal cleaning and shaping. Further research is required in this field in order to obtain an appropriate device that can predict fracture tension of rotative instruments.

REFERENCES:

[1] H.K. Yip, L.P. Samaranayake (1998) *Clin Oral Invest* **2:**148-154.

Class V compomer restorations: the effect of RMGI primers on microleakage

Z. Florita[1], C. Haiduc[1], M. Rominu[1], C. Sinescu[1], R. Rominu[1], A. Kigyosi[1]

[1] *University of Medicine and Pharmacy "Victor Babes" Timisoara, Romania.*

INTRODUCTION: In class V cavities filled with compomers, when the gingival margins are placed in dentine, microleakage nearly always occurs at the interface [1,2]. These results suggest that the efficiency of the adhesive systems to hybridize dentine and cementum must be questioned. It might be suspected that the bonding substrate at the gingival margins contributes less in establishing a micromechanical retention. A series of studies have shown good results regarding resin-modified glass ionomer / dentine interface. The explanation of such behaviour could be the material itself or its primer. Unfortunatelly the resin-modified glass ionomers have poorer clinical handling properties in comparison with either compomers or composites. This study investigated to what extent the use of a polyacid-methacrylate modified primer reduces microleakage in class V compomer-restored cavities.

METHODS: 30 noncarious and crack-free mandibular third molars were used. The teeth were randomly divided into three groups each containing 10 teeth. Class V box-like cavities without any mechanical retention were prepared on each tooth using a rounded fissure diamond bur. The gingival margin was located about 1 mm below the cemento-enamel jonction. The occlusal margin was located in enamel, at 1 mm above the cemento-enamel junction. The prepared cavities were restored as follows: group 1 (HVD) – acid etching 15 seconds (DeTrey Conditioner 36), followed by application of a resin-modified glass ionomer primer (Vitremer Primer – 3M ESPE) and Dyract Extra (Dentsply DeTrey), group 2 (VD) – application of a resin-modified glass ionomer primer (Vitremer Primer), without prior acid etching and Dyract Extra, group no. 3 – application of a resin-modified glass ionomer primer (Vitremer Primer), without prior acid etching and Vitremer. All specimens were thermocycled 1000 cycles between 5-55 ^{O}C. The surface of the specimens were insulated with a double layer of nail varnish except for 1 mm around the occlusal and gingival interfaces. The specimens were stored 24 hours in basic fuchsine 0,5%. All specimens were sectioned along a bucco-lingual plane through the middle of the restorations. To assess dye penetration,the microleakage scores were chosen as follows: 0 - no penetration, 1 - penetration up to 1/2 of the cavity depth, 2- penetration more than 1/2 of the cavity depth, 3 - penetration along the axial wall.

RESULTS: The Kruskal-Wallis test showed statistically significant differences among groups, regarding both cervical ($p=0.012$, $\alpha=0.05$) and occlusal ($p<0.001$, $\alpha=0.001$) interfaces. The median values of microleakage scores were: HVD (cervical-3,occlusal-0), VD (cervical-3,occlusal-1), VV (cervical-3,occlusal-3). For the cervical interfaces Mann-Whitney U tests displayed significant differences among HVD and VD groups ($p=0.03$, $\alpha=0.05$), respectively VD and VV groups ($p=0.03$, $\alpha=0.05$). No significant difference was obtained among HVD and VV groups ($p=1.00$, $\alpha=0.05$). For the occlusal interfaces the Mann-Whitney U tests displayed significant differences among HVD and VD groups ($p=0.005$, $\alpha=0.01$), HVD and VV groups ($p<0.001$, $\alpha=0.001$), respectively VD and VV groups ($p<0.001$, $\alpha=0.001$). A comparison between microleakage at cervical and occlusal in each group, using Mann-Whitney U tests, revealed significant differences for HVD ($p<0.001$, $\alpha=0.001$) and VD ($p=0.07$, $\alpha=0.01$) groups. No significant difference was recorded for the VV group ($p=0.146$, $\alpha=0.05$).

DISCUSSION & CONCLUSIONS: At the cervical (dentine) interfaces, the use of Vitremer Primer, without any prior acid etching, in conjuction Dyract Extra significantly reduces microleakage. At the occlusal (enamel) interfaces the use of Vitremer Primer with prior acid etching, in conjuction Dyract Extra, significantly reduces microleakage. Within the limitations of this study, at both interfaces, Vitremer Primer performs better in association with Dyract Extra than with Vitremer. It could be also noticed that acid etching reduces microleakage for the occlusal (enamel) interfaces, but the effect is opposite for the cervical (dentine) interfaces. The choice between inducing chemical and/or michromechanical adhesion is a challenge and it should be substrate-related.

REFERENCES: [1] S. Hakimeh, J. Vaidyanathan, M.L. Houpt, T.K. Vaidyanathan, S. von Hagen Ziegler (2000) *J Prosthet Dent* **83**:194-203. [2] S.K. Sidhu, J.F. McCabe (2004) *Am J Dent* **17**:327-330.

Expansion of Adult Human Chondrocytes on an Extendable Surface: A Strategy to Reduce Passageing-Related Dedifferentiation

D. Vonwil[1], A. Barbero[1] T. Quinn[2], I. Martin[1]
[1] *Dept. of Surgery and of Research, University Hospital, Basel, Switzerland*
[2]*Cytomec GmbH, Spiez, Switzerland*

INTRODUCTION:

Cell-based cartilage tissue engineering approaches generally require chondrocytes from a small biopsy to be expanded in monolayer culture. However, prolonged culture and passaging is associated with de-differentiation and subsequently reduced capability to produce functional cartilage tissue [1].
Instead of letting cells to grow confluent before plating them into a bigger culture dish, continuously providing cells more space as they grow reduces the need for passaging. By using a novel system with an extendable growth surface to culture chondrocytes**,** we would like to test the hypothesis that lower **passaging number would better maintain the chondrocytic phenotypes and enhance their post-expansion chondrogenic capacity.**
Before we can address this main question, appropriate conditions for expanding chondrocytes on extendable surfaces must be found.

METHODS:

Adult human articular chondrocytes (AHAC) of one donor were seeded on an extendable, Collagen I (Coll I) functionalized poly dimethyl siloxane (PDMS) membrane [2]. AHAC were allowed to attach for 24 h before the membrane surface area was isotropically extended at a rate of 4% every 4h using a Cellerator (Cytomec GmbH). This device consists of a motorized iris-like mechanism which holds the PDMS membrane. Membrane expansion is thereby automated [3].
Control static conditions were Coll I coated PDMS membranes, uncoated and Coll I coated tissue culture treated plastic dishes (TCPS).

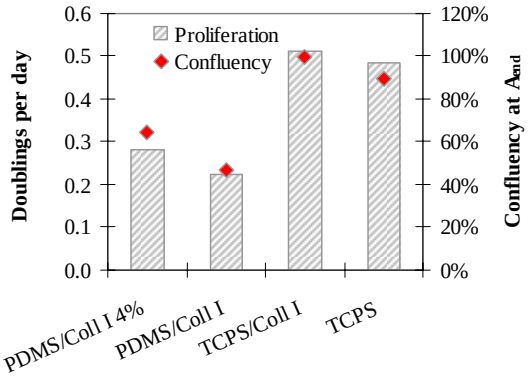

Fig. 1 Cell Proliferation and Confluency

RESULTS:

On the extendable Coll I functionalized PDMS surface, AHAC attachment was as quantitative as on TCPS surfaces. However, on the functionalized PDMS membranes, AHAC proliferation rate was reduced nearly of two fold. Importantly, AHAC cultured on functionalized PDMS membrane under surface extension proliferated with 1.3-fold higher rate than those statically cultured on Col I coated PDMS membrane (**Fig. 1**).

DISCUSSION & CONCLUSIONS:

These preliminary results show that it is feasible to expand AHAC on an extendable surface (total area increase: 300%). Ongoing experiments are aimed at investigating if such culture technique by enabling to reduced/avoid cell passaging, could better maintain the chondrocytic phenotype and enhance the chondrogenic capacity of AHAC as compared to standard monolayer culture conditions.

REFERENCES:

[1] E. M. Darling & K. A. Athanasiou, J Orth. Res., 23 (2005) 425-432. [2] Communication by B. Hinz, EPFL. [3] http://www.cytomec.com

Effects of Texture of Austenitic Stainless Steels on Pitting and Crevice Corrosion

P.Y. Eschler[1], R. Ziegenhagen[2], H. Lüthy[3], L. Reclaru[1],

[1]PX Holding SA, La Chaux-de-Fonds; [2]Cartier Horlogerie, La Chaux-de-Fonds ; [3]University of Basel

INTRODUCTION

The aim of this study was to assess the corrosion behaviour of austenitic stainless steels used in medicine and dentistry according to the orientation of analyzed surfaces. The corrosion phenomena studied are localized pitting corrosion and crevice corrosion.

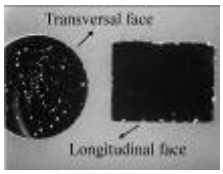

Fig. 1: Specimen #1 after 2 h in $FeCl_3$ at 50°C.

METHODS

Table I. Austenitic stainless steels tested.

#	DIN	AISI	ASTM
1	1.4571	316L Ti	--
2	1.4435	316 L	--
3	1.4441	316 L Med	F138
4	1.4539	904L	--

Pitting resistance by the use of ferric chloride solution (ASTM G48).

After immersion of samples in $FeCl_3$ 0.5 M during 2 h at 50°C, the pitting density is then estimated for every face (transversal and longitudinal) (fig.1).

Evaluation by electrochemical techniques (ASTM G3 ASTM G59)

The test medium is an electrolyte based on the EN 1811 standard (1 ± 0.001 g/l of urea, 5 ± 0.001 g/l of NaCl, 940 ± 10 µl/l of racemic lactic acid, with a pH of 4.5).

General corrosion and pitting corrosion

Investigated electrochemical parameters were open circuit (E_{oc}) in the N2-deaerated electrolyte for 16h, plotting of the polarization curve (± 150 mV vs. E_{oc}), plotting of the overall polarization curve (-1000 mV to +1000 mV) and coulometric analysis by zone.

Crevice corrosion

The test procedure is described in the ASTM F746.

RESULTS

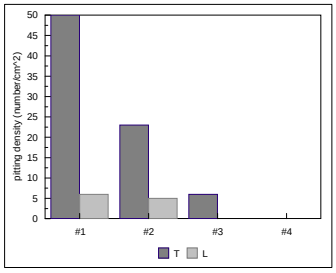

Fig. 2: Pitting test on transversal and longitudinal faces. Test medium 0.5 M $FeCl_3$ at 50°C, 2 hours.

Table II. I_{corr} and coulometric analysis on transversal (T) and longitudinal (L) faces.

	i_{corr} .[µA/cm^2]		Coulometric analysis			
			E_{corr}-300mV (mC/cm^2)		E_{corr}-600mV (mC/cm^2)	
	T	L	T	L	T	L
#1	0.46	0.27	557	192	10670	3523
#2	0.06	0.02	3.0	27.0	198.0	106.0
#3	0.91	0.72	4.8	2.5	1100.0	53.0
#4	0.09	0.06	2.5	1.3	21.0	11.0

$E_{crevice}$ (mV)		
	T	L
#1	-225	-200
#2	50	100
#3	25	75
#4	100	350

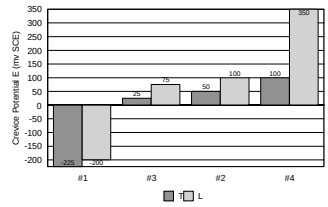

Fig. 3. Crevice potential values measured on the transversal (T) and longitudinal (L) faces.

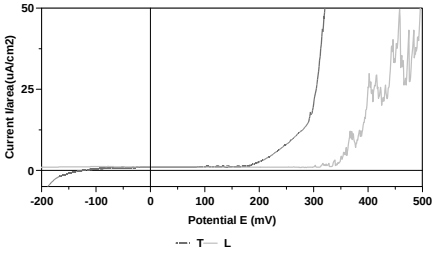

Fig. 4. Potentiodynamic polarization curves on linear axes plotted for the transversal and longitudinal faces for specimen #2.

DISCUSSION & CONCLUSIONS

Surfaces oriented perpendicular to the drawing/rolling direction (transversal faces) are consistently more prone to corrosion than surfaces in the parallel direction (longitudinal faces).

PULP CHAMBER TEMPERATURE VARIATIONS USING THREE TYPES OF LIGHT CURING UNITS

C. Haiduc[1], D. Dodenciu[1], C. Sinescu[1], M. Negrutiu[1], G. Draganescu[2], V. Mara[3]

[1] *University of Medicine and Pharmacy "Victor Babes" Timisoara, Romania*

[2] *Polytechnics University of Timisoara Romania,*

[3] *Columbia University, USA*

INTRODUCTION: In light cured composite resins, a light source of adequate intensity and wavelength from 400 to 500 nm activates camphorquinone with peak absorption at 468 nm. Three essential components are required for an adequate polymerization: sufficient radiant intensity, correct wavelength of the visible light and optimum curing time. Other factors such as type of composite resin, shade and translucency, temperature of the composite material [1], thickness of the increment, distance of the light tip from the surface of the material, curing time and post-irradiation time [2], also influence the depth, and therefore the efficiency of polymerization.

METHODS: For determining the pulp chamber temperature, a KTY 11-6 Infineon traductor was inserted. The main advantages of this traductor are: the reduced size (2,1/1,9 mm), weight (0,02 g), linear output, excellent long term stability, fast responding time. A class I cavity was prepared in an extracted molar, leaving a 1 mm thick dentin layer between the pulp chamber and the bottom of the cavity. The cavity walls were divergent to allow the filling to be taken out. A 2 mm composite resin (the same in each sample) layer was applied into the cavity and light cured. For the reproducibility process a mark was done on the tooth cavity walls in order to maintain the 2 mm composite layer. No etching or bonding materials were used. Taking out the filling was done by high speed drilling in permanent cooling and sharp instruments for leaving a 1mm thick dentin layer between the pulp chamber and the bottom of the cavity. The curing units used were: halogen unit (Degulux, Degussa), LED (Bluphase C5, Vivadent and MiniLed, DeTrey Dentsply) and plasma unit (Apollo 95E, DMDS). 20 seconds were considered for the curing procedure for halogen and LED curing units and 6 seconds for the plasma unit.

RESULTS: Measurements of the pulp chamber temperature were done in every second for each type of curing light unit, untill the temperature reached a constant level. The results of the temperature measurements were mediated in order to obtain as realistic values as possible.

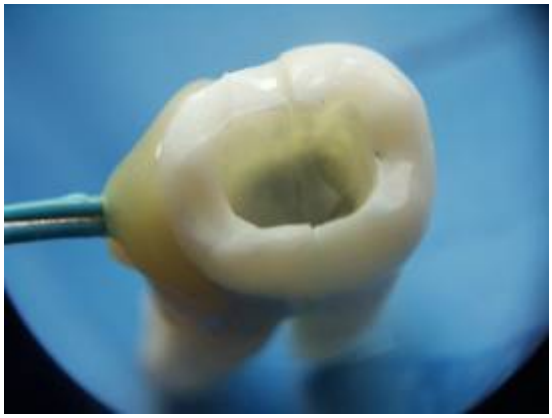

Fig. 1. The tooth with the traductor inserted in the pulp chamber.

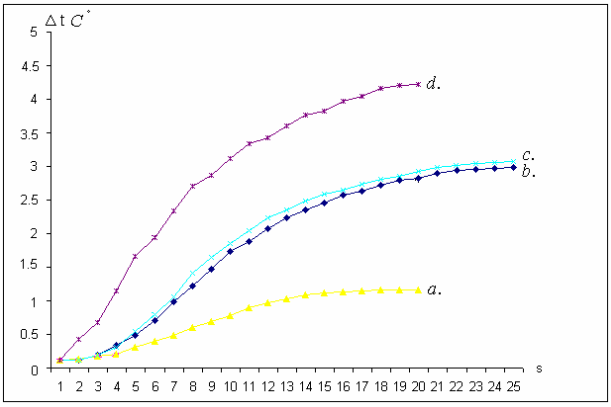

Fig. 2. The graphic represents the pulp chamber variation temperature until the maximum is achived. Temperature variation in pulp chamber for: a –Apollo 95E; b – Bluphase C5; c –MiniLed; d – Degulux .

DISCUSSION & CONCLUSIONS: The results obtained with this type of traductor points out a higher risk of overheating the pulp chamber when halogen lamps are used, compared to the LED curing units (fig. 2). The plasma curing unit induced the lowest temperature variation, being the minimal invasive curing device from the selected ones.

REFERENCES:

[1]B. Bennett, A. Puckett, D. Pettey, B. Roberts, (1994) *J Dent Res* **73**:227.

[2]R. Blankenau, R. Erickson, F.A. Rueggeberg (1999) *Compendium* **20:**122.

THE ANALYSIS OF REMOVABLE PARTIAL DENTURES WITH CLASPS MADE FROM THERMOPLASTIC AND CHEMOPLASTIC MATERIALS. A BIOMECHANICAL APPROACH OF THE INTERFACE BETWEEN CLASPS AND DENTURE.

M. Negrutiu[1] , C. Sinescu[1], C. Sticlaru[2], A. Davidescu[2], M. Rominu[1]
[1] *University of Medicine and Pharmacy "Victor Babes" Timisoara, Romania*
[2] *Polytechnics University of Timisoara Romania*

INTRODUCTION: One of the most recent advances in dental technology is the application of nylon-like materials for the fabrication of dental appliances. This material (Flexite, Flexiplast, ValPlast) generally replaces the metal, and the pink acrylic denture material used to build the framework for standard removable partial dentures (RPD) [1]. It is nearly unbreakable, is pink-coloured like gums, can be built quite thin, and can form not only the denture base, but also the clasps as well. Since the clasps are built to curl around the necks of the teeth, they are practically undistinguishable from the gums [2].

Fig.1. The mechanical scanner used in this study.

METHODS: The purpose of this study is to analyse the behaviour of removable partial dentures with clasps, by comparing the thermoplastic material to the chemo plastic one. Therefore, numerical simulation analysis method based on ProEngineer and Ansys software was used. The modelling of the removable partial denture with clasps was made using mechanical scanning systems, Micro Scribe G2 (Fig.1). The RPD meshing procedure resulted in 3404 nodes connected in 1578 elements (Fig.2). The loading of the RPD was done with a force of 1200 N on the entire structure.

RESULTS: The study points out the tensions appeared in removable partial denture with clasps for each situation that was considered. The maximum equivalent (Von Mises) stress (7,114 Pa) recorded in the chemo plastic RPD was significantly higher compared to those in the thermoplastic one (5,248Pa) (Fig.3). The total maximum deformation recorded in clasps for Chemo plastic RPD was 0,742 mm, while the thermoplastic one was 0,748 mm.

DISCUSSION & CONCLUSIONS: The thermoplastic resins have been used in dentistry for over 50 years and their applications continue to develop. Theese materials have superior properties and characteristics; therefore they provide excellent esthetics and biocompatibility. As a general conclusion the injection method of the thermoplastic materials brings more advantages in the behavior of the removable partial dentures with clasps, compared with the conventional technology.

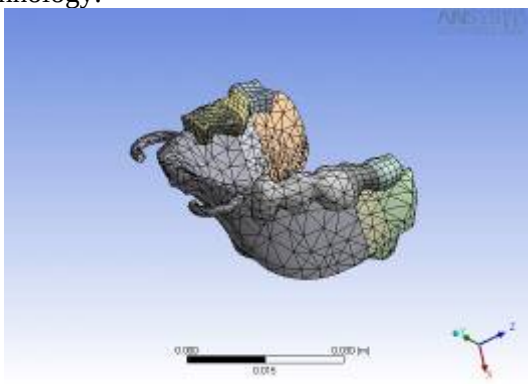

Fig.2. Meshing the injected RPD.

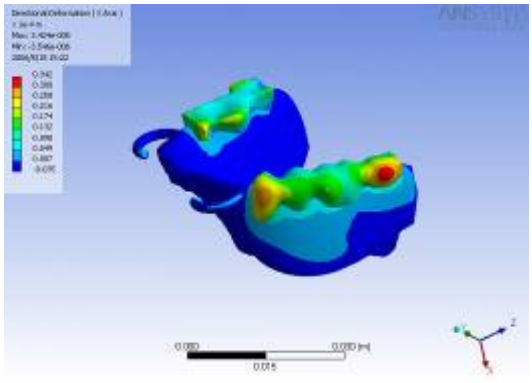

Fig. 3. The tensions in the clasps and in the RPD.

REFERENCES: [1] A E.Amin (1995) *Egypt Dent J* **41**(3):1299-1304. [2]J. John, S.A. Gangadhar, I. Shah (2001) *J Prosthet Dent* October.

OPTIMIZATION OF PHYSICAL PARAMETERS IN LASER WELDING PROCEDURE FOR FIXED PARTIAL DENTURES TECHNOLOGY

M. Negrutiu[1] , C. Sinescu[1], M. Rominu[1], G. Draganescu[2]
[1] *University of Medicine and Pharmacy Timisoara "Victor Babes", Romania*
[2] *Politechnics University of Timisoara, Romania*

INTRODUCTION: The laser welding procedure has become a widely used method in dental laboratory, having many advantages in time saving, strength, insertion axis and marginal adaptation optimization [1]. Thus, looking at the available literature, many experiments have been made since 1970; they focused on non precious and precious alloys and have shown contradictory results, due to the experimental procedures based on different laser parameters [2]. In this study, the weld ability of two non precious alloys was investigated.

METHODS: For this study two types of metal infrastructures were casted, two made of Co-Cr (three units bridge) and two of Ti (four units bridge). For the Co-Cr, one of the specimens remains intact; while in the other two defects were made: one crown was shortened in the cervical area and the other crown was cut in half. For the Ti bridge, one was left intact; in the other one a cutting in a half of the entire bridge was made. The procedure consists in determining the appropriate welding parameters that could lead to a joining in depth without cracks or gas entrapments in the welding area (Fig. 1). The alloy's ability to weld was evaluated with Nd-Yag Laser equipment (Orotig). The laser was activated in a pulsed mode. The efficiency of the welding was measured with tensile tests. In order to evaluate the welding, metallographic examinations and X-Ray microprobe analysis were performed through the welded area and compared with the intact ones.

Fig. 1. The parameters used in Co-Cr welding.

RESULTS: The Co-Cr alloy presents an excellent welding ability (Fig. 2). A very important change in the microstructure was determined, due to the laser effect in the welding area, increasing its micro-hardness. Titanium also presents a very good welding ability, but the micro-hardness in the welding zone is lower. (Fig.3).

Fig.2. Co-Cr fixed partial denture welded with laser

Fig. 3. The Titanium bridge after welding.

DISCUSSION & CONCLUSIONS: The micro-structural changes in the welding area cannot be avoided, due to the very fast cooling process after laser welding, and cannot be restored with an adequate thermal treatment. The excellent welding capacity of Co-Cr alloy is usefull when used in casting dental prosthesis with complex design compared with titanium.

REFERENCES:

[1]T. Fusayama, S. Wakumoto, H. Hosoda (1964). *J Prosth Dent* **14**:334-342. [2]H. Apotheker, I. Nishimura, C. Seerattan (1984) *Lasers in surgery and medicine* **4:**207-213.

Fibrin delivery of molecular variants of fibronectin central cell-binding domain that provide integrin-specific instructions to mesenchymal stem cells

Mikaël Martino[1], Mayumi Mochizuki[1], Michael Smith[2], Jeffrey A. Hubbell[1] and Thomas Barker[1,3]
[1]Inst. for Bioengineering, Swiss Federal Inst. of Technology Lausanne, Lausanne,, Switzerland; [2]Dept. of Materials, Swiss Federal Inst. of Technology Zurich, Zurich, Switzerland; [3]Wallace H. Coulter Dept. of Biomedical Engineering, Georgia Inst. of Technology, Atlanta, United-States.

Introduction: Fibrin is an ideal protein/cell delivery vehicle for repairing damaged tissues since the polymer is derived from the normal haemostatic pathway. Contaminating fibronectin (FN), a multidomain extracellular matrix (ECM) protein present in fibrinogen preparations, is in part responsible, through its central cell-binding domain, for cell attachment to fibrin gels. FN has recently been shown to stimulate proliferation or differentiation through modulation of integrin binding affinities[1]. One example of modulation is the binding of $\alpha_5\beta_1$ integrin, which requires binding to the Synergy sequence (PHSRN) on the 9th Type III repeat and RGD on the 10th Type III repeat, versus $\alpha_v\beta_3$ integrin requires only RGD. We hypothesized that the integration of variants of the 9th and 10th Type III repeats with different integrin binding affinities into fibrin matrix in the place of FN would provide more specific instructions that would direct human mesenchymal stem cell (MSC) proliferation or differentiation.

METHODS: *FN domains:* The 9th and 10th Type III repeats (FN III10 and FNIII9-10) were cloned into the pGEX4T-1 expression vector. Addition of the α_2-plasmin inhibitor transglutaminase-sensitive sequence at the N-terminus allows covalent crosslinking into fibrin gels[2]. A point mutation of Leu^{1408} to Pro (FN III9*-10) was made to increase the specificity for $\alpha_5\beta_1$ integrin[3]. Protein were produced in *E.coli* BL21 and purified with an *ÄKTA*FPLC. *Attachment and integrin specificity:* MSCs were plated on ECM-coated plate and allowed to attach with or without functional blocking antibody (FBA) for the integrin $\alpha_5\beta_1$ and/or $\alpha_v\beta_3$. Adherent cells were quantified with crystal violet. *Spreading assay:* Electrical Cell Impedance Sensing was used to determine spreading rates of MSC on ECM-coated electrodes. *Proliferation and differentiation in 2D:* MSCs, were plated on ECM-coated plate with or without $\alpha_5\beta_1$ or $\alpha_v\beta_3$ FBA in normal or osteo-inducer media. Cell number was quantified with Alamar blue after 4, 7, 14, and 21 days. Alkaline phosphatase (ALP) activity was determined with p-nitrophenyl phosphate. *Proliferation and differentiation in fibrin gel:* Fibrin polymers were made to obtain 5 molecules of fibrinogen per molecule of FN domains. MSCs were seeded into the matrices with or without FBA and osteo-inducer media. Cell morphology, cell number and ALP activity were quantified as in 2D.

RESULTS: FN, FN III9-10, and FN III9*-10 showed the highest binding and spreading rates. FN III10, despite poor initial cellular attachment, displayed near-equivalent spreading rates to full-length FN, whereas fibrinogen demonstrated poor cellular attachment and low spreading kinetics. Attachment assays with FBA confirmed the specificity of FN III9-10 and FN III9*-10 for the integrin $\alpha_5\beta_1$ (FN III9*-10 > FN III9-10), whereas FN III10 showed poor specificity for both $\alpha_v\beta_3$ and $\alpha_5\beta_1$ integrins. In 2D, the proliferation on FN, FN III9-10, and FN III9*-10 was significantly better than on FN III10. Assays with FBA demonstrated that $\alpha_5\beta_1$ was implied in these differences. MSC differentiation into osteoblasts was significantly accelerated on the recombinant FN domains compared to FN and fibrinogen (FN III9*-10 > FN III9-10 > FN III10 > FN > fibrinogen). Again, $\alpha_5\beta_1$ FBA was capable of significantly reducing the differentiation. Delivering FN domains into fibrin gels displayed small differences for MSC proliferation within the first week, and $\alpha_5\beta_1$ FBA significantly reduced proliferation while $\alpha_v\beta_3$ FBA increased it. As in 2D, differentiation was significantly accelerated in gel containing FN domains compared to FN and fibrin only, and $\alpha_5\beta_1$ FBA was able to decrease these differentiation events while $\alpha_v\beta_3$ FBA increased them.

DISCUSSION & CONCLUSIONS: FN replacement by FN domains provides more specific instructions to MSC by directing proliferation or differentiation while maintaining similar attachment and spreading capacities of the full length protein. Cell-matrix interactions through $\alpha_5\beta_1$ were implied in these differences. This new generation of fibrin matrix could be used alone or in combination with other differentiation factors, such as growth factors, for cellular processes that require specific integrin binding.

REFERENCES:

[1]Stephansson SN *et al*. Biomaterials. 2002 23(12):2527-34. [2]Schense JC and Hubbell JA. Bioconjug Chem. 1999 Jan-Feb;10(1):75-81. [3]Altroff H *et al.* J Biol Chem. 2003 Jan 3;278(1):491-7.

Novel screening protocol for wet chemical surface functionalization

S.Saxer[1], S.Zürcher[1], S.Tosatti[1], K.Gademann[2], M.Textor[1]

[1] ETH Zurich, Zurich, Switzerland. [2] EPF Lausanne, Lausanne, Switzerland.

INTRODUCTION: The arising diversity of biomaterials requires custom-made surfaces that offer application-specific properties. Often surface modification is used to ease an assimilation of the bulk material in different environments and prevent degradation[1]. To ensure an adequate surface modification, a firm surface chemistry is needed, which is stable enough to withstand changing conditions over the whole time period. The present work aims on the development of novel binding motifs on the basis of natural adhesives, which shows the extraordinary ability to strongly attach onto various materials[2,3]. The potential adhesion of differently functionalized amino acids should be tested under various conditions and surfaces. The high number of experiments requires a novel screening protocol for effective and simultaneous testing. Therefore a multi-well array was designed and verified with a fluorescence-based read out.

METHODS: The verification of the multi-well array is done by the adsorption of poly (L-lysine)-*grafted*-poly (ethylene glycol) solutions (PLL-*g*-PEG) in HEPES II buffer. The adsorption is then analyzed by microspot ellipsometry (Sentech SE8500, 350-920nm, spot size; <1mm) and/or by the fluorescence microscope (Zeiss Axioscope 2plus).

RESULTS: The designed multi-well array is able to perform simultaneously eighty adsorption experiments, each with a volume of 20µL (Fig. 1). The functionality of the array was tested on glass slides and coated/uncoated silicon wafer, whereas PLL-*g*-PEG served as an adhesion model, to coat and protect the surface. The quality of this adsorption was then verified with a secondary incubation of FITC-fibrinogen, on top of the PLL-g-PEG layer, followed by measuring the fluorescence intensity (Fig. 2). It shows an increasing FITC-fibrinogen adsorption with decreasing PLL-*g*-PEG layer thickness.

Fig. 1: Multi-well array for parallel-adsorption on various surfaces

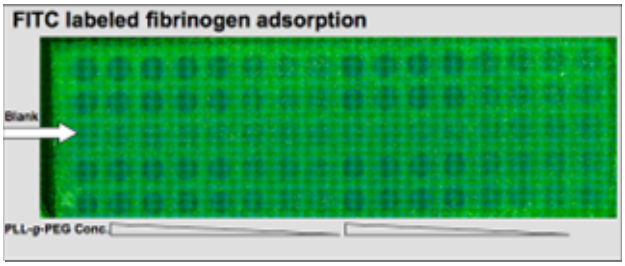

Fig. 2: Fluorescence microscope picture of the multi-well array (SiO_2-surface) after incubation with differently concentrated PLL-g-PEG and FITC labeled fibrinogen solutions.

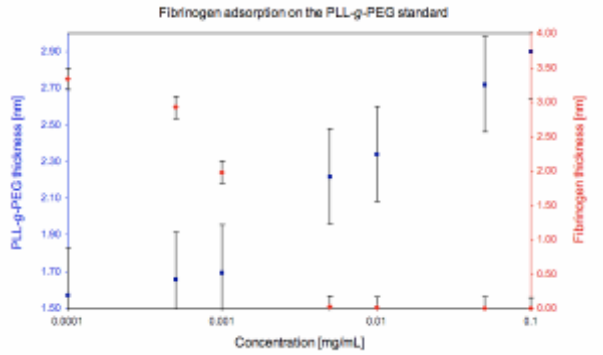

Fig. 3: Measurement of the PLL-g-PEG layer thickness versus the FITC-fibrinogen layer on silicon oxide by microspot ellipsometry

Furthermore the adsorption studies were also confirmed by µspot ellipsometry (Fig. 3).

DISCUSSION & CONCLUSIONS: The fluorescence measurements offer a very fast, semi-quantitative verification of the adsorption properties of different molecules. In addition this data can always be investigated more precisely by µspot ellipsometry, as a secondary method. In the near future new potential adhesive molecules should be linked onto PLL-*g*-PEG and investigated by using the multi-well array.

REFERENCES:

[1]Castner, D. G.; Ratner, B. D. (2002) *Surf. Sci.* 500:28-60. [2]Waite, J. H. (2002) *Integr. Comp. Biol.* 42: 1172-1180. [3]Zürcher, S., Wäckerlin, D., Bethuel, Y., Malisova, B., Textor, M., Tosatti, S., Gademann, K. (2006) *J. Am. Chem. Soc.* 128: 1064-1065

Diamine biomolecules surface functionalization single-walled carbon nanotube as gene-delivery vector

C.Y. Li[1], C.K. Hsu[1], F.H. Lin[2], L. Stobinski[3]

[1] Department of Material Science and Engineering,National Taipei University of Technology,Taipei,Taiwan

2 Department of Biomedical Engineering,National Taiwan University, Taipei, Taiwan.
3. Polish Academy of Sciences, Institute of Physical Chemistry, Warszawa, Poland

INTRODUCTION: The single-walled carbon nanotube is at the same scale with DNA that the aromatic rings on surface of CNT can directly combine together with ring structure on DNA molecules through the electron exchanging and inducing the π-πstacking force in between[1,2]. In this study we use the commercialized single-walled carbon nanotube to combine with two different kind of biocompatible molecules after purification. The molecules are putrescine and polyoxyethylene bis-amine to form complex with plasmid DNA, EGFp-C1 is selected for direct expression, and evaluate the in vitro properties...

METHODS: Computer simulation with Hyperchem was first devoted to predict the stability of this system. 14 start codons of EFFP-C1 was selected to build a single-stranded DNA (ssDNA) and combine with chiral form single-walled carbon nanotube (SWCNT) with length 10nm. The formation energy was calculated. physical experiments contains the examination of ssDNA-SWCNT complex with Raman spectroscopy and the surface modification of SWCNT by diamine biomolecules. The surface-modified SWCNT was analyzed with FTIR, TGA and TEM. Bioassay was the last part to evaluate the biocompatibility and transfection efficiency. LDH, MTT, total DNA and IL-6 release were done to fully estimate the bioproperties of these materials. HeLa and 3T3 were chosen as transfection host to justify the transfection efficiency.

RESULTS:

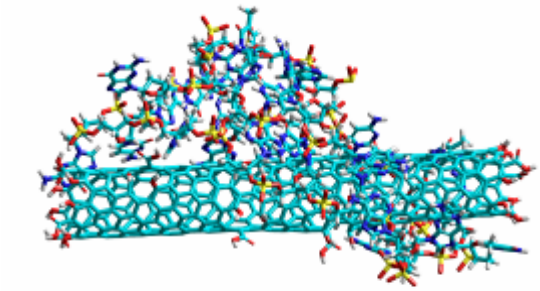

Fig.1 Complex of ssDNA-SWCNT showing the wrapping of ssDNA around SWCNT and having a great stability.

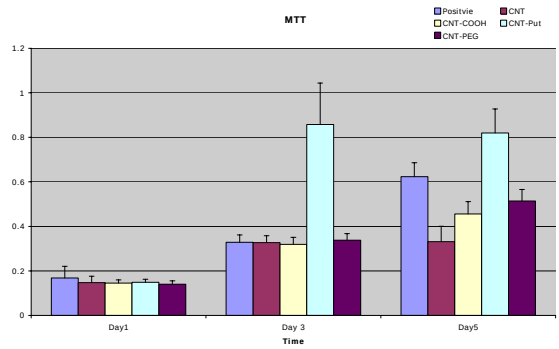

Fig.2 MTT result gives the direct evidence that surface-modified SWCNT can enhance the activity of cells.

DISCUSSION & CONCLUSIONS: Computer simulation indicates that the ssDNA-SWCNT complex can form spontaneously and with a great stablility through surface interaction. The Raman spectroscopy further proved the wrapping geometry of this complex. Surface-modified SWCNT can bind to DNA selectively with different surface functional groups. A series of bioassay promote the idea that diamine surface-modified SWCNT have a good biocompatibility and inspire the cell growth. In-vitro transfection did not show a great result as expected which may due to the insufficient functional groups on the surface of SWCNT

REFERENCES: [1]M.Zeng et al.,*Science* ,302(2003),1545-1548. [2] R. K. Castellano, F. Diederich and E. A. Meyer, Angew. *Chem. Int. Ed.* 42, 11(2003),1210-1250

ACKNOWLEDGEMENTS: The completion of this research should give special thanks to Department of Biomedical Engineering, National Taiwan University and Graduate Institute of Manufacturing Technology, National Taipei University of Technology.

Optimization of operator parameters for microplasma welding of dental alloys

L. Sandu[1], F.Topală[1],V. Bârdeanu[2], C. Borțun[1]

[1] "V. Babeş" University of Medicine and Pharmacy Timişoara, Romania, [2] National R&D Institute for Welding and Materials Testing Timişoara, Romania

INTRODUCTION: The success of welding procedures in dental alloys depends on the operator's control of different parameters (1, 2). The study investigated the effect of the welding parameters on the microstructure of the cast and compared the results of different casting alloys.

METHODS: Cast Co-Cr-Mo alloys plates were prepared for experimental welding tests. After polishing the surfaces to be welded, the plates were matched and welded using microplasma. Each specimen was bilaterally welded in a butt joint configuration, with a spot overlapping of more than 50% (Fig. 1).

Fig. 1. Microplasma welded plates.

The joints were analyzed macroscopic and radiographic. After that micrographic observations perpendicular to the weld axis were conducted in order to analyse the quality of the microstructure. Additionally, the microhardness was measured both in the welded and the heat-affected zones and than compared to the non welded cast alloy.

RESULTS: The welding imperfections, like an nonuniform width of the welding rib, craters on the welding surface, associated with radial cracks, lack of melting between the components have to be detected, explained an eliminated (Fig. 2).

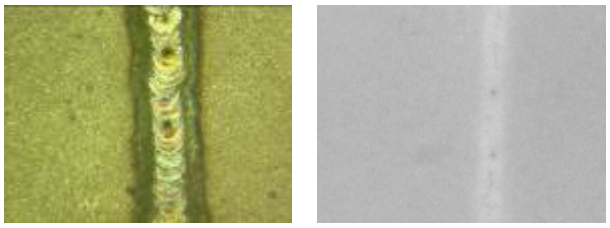

a *b*

Fig. 2. Macroscopic (a) and radiographic (b) aspect of the welded area.

The areas with increased microhardness values, located in the heat affected zone are fragile structures. Associated with welding defects, like voids and cracks can lead to an early degradation of the welded structure (Fig. 3). Adequate combination of the welding parameters appears to improve the success of the welding procedure. Operator skill is also an important variable.

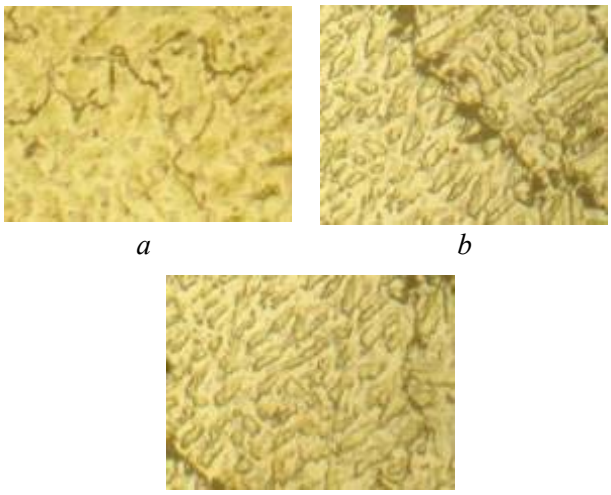

a *b*

c

Fig. 3. Microstructure of the welded area (a), heat affected zone (b) and cast alloy (c).

DISCUSSION & CONCLUSIONS: Cracks and modifications of the microstructure due to the rapid heating and solidification process can be a real problem and affect the quality of the joint. The cast alloys showed a dendritic microstructure, but the microstructure of the welded areas appeared very fine, as a result of the very rapid solidification process. The control of the welding parameters is determinant for the weld quality and the influence of the operator skill can be reduced by their optimization.

REFERENCES: [1] C. Bertrand, Y. Le Petitcorps, L. Albingre, V. Dupuis (2004) *Optimization of operator and physical parameters for laser welding of dental materials*, Br Dent J, 196(7), pp. 413-418. [2] C. Bertrand, Y. Le Petitcorps, L. Albingre, V. Dupuis (2001) *The laser welding technique applied to non precious dental alloys procedure and results*, Br Dent J, 190(5), pp. 255-257.

ACKNOWLEDGEMENTS: This study was supported by the Grant CEEX-ET 5865/2006 from the Ministry of Education and Research, Romania.

Three dimensional teeth designs generated by NURBS modeling

L. Sandu[1], F.Topală[1], N. Faur[2], C. Borțun[1]

[1] "V. Babeş" University of Medicine and Pharmacy Timişoara, Romania, [2] Politehnica University Timişoara, Romania

INTRODUCTION: Nonuniform rational B-spline (NURBS) is a mathematical model commonly used in computer aided design, manufacturing and engineering. It was introduced in dentistry through CAD/CAM systems. CAD is mainly used for detailed 3D models but it is also used throughout the manufacturing process, from conceptual design, through strength and dynamic simulation analyses. The aim of the study was to achieve 3D models in order to develop applications for didactic and basic research use, to design and optimize dentures or denture components.

METHODS: For most situations, a single scan will not produce a complete model of the object. Multiple scans, from many different directions are usually required to obtain information about all sides of the object. Therefore different normal plaster teeth were scanned rotary and from a single plane using a laser scanner PLX 1200.These scans were brought in a common reference system, a process that is usually called alignment, and then merged to create a complete model. Resulted files were imported in Rhinoceros NURBS modeling program, were the point clouds from the teeth surfaces were cleaned and assembled. The collected data were used to construct three dimensional models. These points were used to extrapolate the shape of the subject, a process called reconstruction (Fig. 1). Reconstruction involves finding and connecting adjacent points in order to create continuous surfaces.

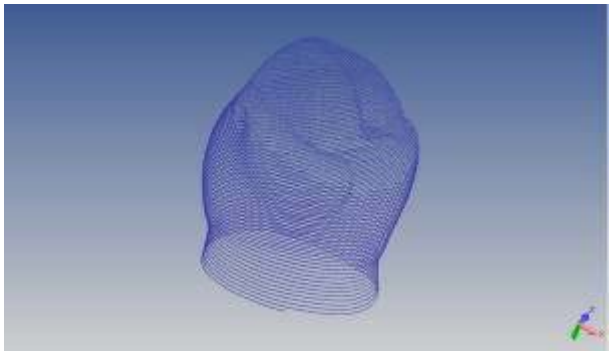

Fig. 1. Point clouds from the teeth surface.

Because of the complex teeth geometry, a nonparametric program was chose for modeling. The parts resulted from the scanning were assembled by the superposition of the points. After that a triangular mesh was constructed as uniform as possible, using Open Source programs. Surfaces and solids were generated.

RESULTS: NURBS modeled resulted solids (Fig. 2) have a properly designed morphology and can be used for a wide variety of applications.

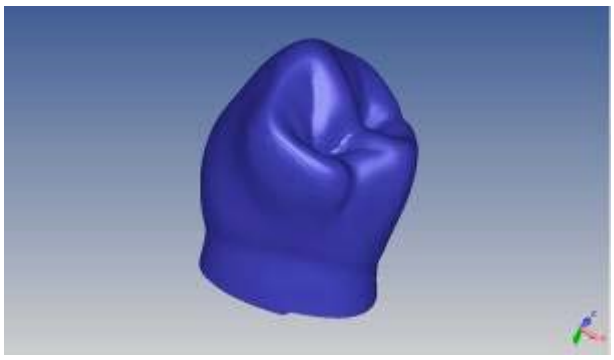

Fig. 2. Three dimensional model of a premolar.

DISCUSSION & CONCLUSIONS: The working methods are laboriously, they involve a lot of working steps and specific knowledge. They can be used in a wide variety of applications, for finite element analyses, for computer aided machines and for didactic purpose. The exactness of the models obtained by three dimensional scanning is higher than those obtained using other modeling methods.

REFERENCES: [1] P. Ausiello, A. Apicella, C. L. Davidson, S. Rengo (2001) 3D–finite element analysis of cusp movements in a human upper premolar, restored with adhesive resin-based composites, Journal of Biomechanics, 34, pp. 1269–77. [2] L. Sandu, N. Faur, C. Borțun (2003) *Finite Element Analysis of Stress Distribution in the Abutment Teeth involved in the Treatment with Removable Partial Dentures.* Proceedings of the 6th International Conference on Boundary and Finite Element, Ed. Politehnica, Timişoara, pp. 189-94.

ACKNOWLEDGEMENTS: This study was supported by the Grant CEEX-ET 5865/2006 from the Ministry of Education and Research, Romania.

Reverse Enginering and Finite Elements Analysis In Removable Partial Denture.

C. Bortun[1], A. Cernescu[2], N. Faur[3], L.Sandu[4], F. Topala[5]

[1,4,5]*„Victor Babes" University of Medicine and Pharmacy, Timisoara, Romania*
University School of Dentistry, Specialization of Dental Technology , [2,3]*Politehnica University Timisoara, Mechanical Engineering Faculty, Department Strenght of Material*

INTRODUCTION: The finite element analysis is well known in dentistry. In the field of removable partial dentures were studied dental clasps, major connectors and other maintaining, support and stabilization systems [1,2]. The objective of the study is to test wax pattern framework optimum design of removable partial denture (RPD) using **numerical simulation**. After testings, the pattern can be transformed into finite piece.

METHODS: There was made a comparation between "LiWa" (WP Dental, Beven/Hamburg Germany) wax pattern and different CoCrMo metallic frameworks. Those were 3D laser scanned with LPX 1200 (Roland) and processed with Dr. Picza program (Fig. 1).

a. b. c d. e.

Fig.1 3D scanned wax pattern: a. "LiWa" wax pattern; b. metallic framework; c,d. scanner, e. 3D scanned wax pattern.

Further processing were made using ,,Pixform Pro''(Roland) program. Imported point clouds were processed and transformed into one surfaces network after connection. This network was exported as DXF extension file in CAD program, where the 3D model (Solid Work 2007 - SolidWork Corporation West) of the pattern was obtained.

RESULTS: Within the analyses results made on patterns, meshing and loading of some prosthetic pieces fragments was allowed. As fragments, RPD clasps were chosen. In the second figure are presented some of the results.

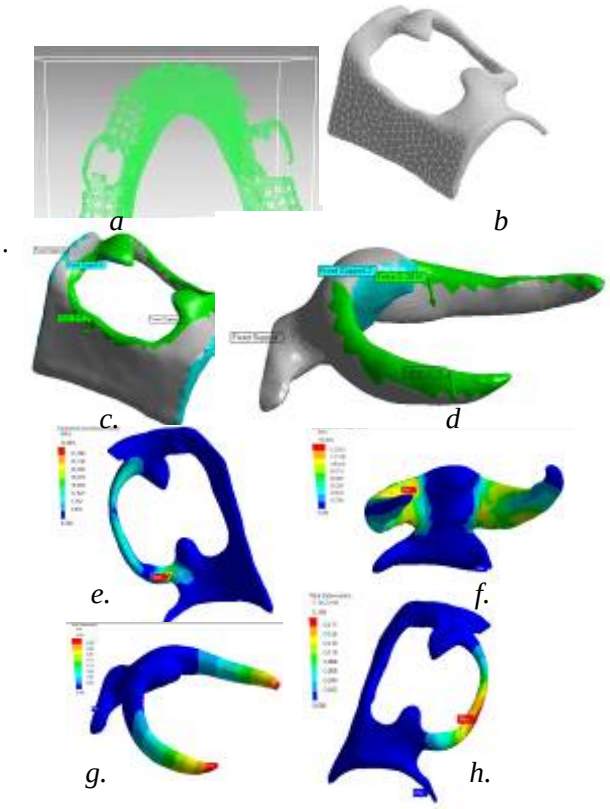

Fig.2 a. RPD point clouds – wax pattern; b. circumferential clasps meshing; c,d. fixed support conditions; e,f. von Misses equivalent stresses; g,h. clasps total deformation.

DISCUSSION & CONCLUSIONS:

1. Using light curing waxes is a novelty in the field of removable partial dentures technology.
2. Wax pattern finite element analysis allows the design testing of future metallic frameworks of RPDs, before their achieving.

REFERENCES: [1]Sato Y, et all. (1995) *An Investigation of Preferable Taper and Thickness Ratios for Cast Circumferential Clasp Arms Using Finite Element Analysis,* Int J Prosthodont, 8:392-397. [2]Sandu L, Faur N, Borţun C. (2007) *Finite element stress analysis and fatigue of cast circumferential clasps*.J. Prosthet. Dent., 2007 vol. 97, no.1: 39-44.

ACKNOWLEDGEMENTS: This study was supported by the CNCSIS Grant, no.744/2006, from the Ministry of Education and Research of Romania

EXPERIMENTAL RESEARCHES ABOUT TECHNOLOGICAL AND MICROSTRUCTURAL ASPECTS IN THE CASE OF COBALT-CHROMIUM DENTAL ALLOYS

Antoniac Petrut[1], A. Ivanov[1], I. Antoniac[1], F. Miculescu[1], G. Cosmeleata[1]

[1] *University Politehnica of Bucharest, Romania.*

INTRODUCTION: In present paper there are presented the results of microstructure investigations on samples of partial removable denture made of cobalt-chromium dental alloys and some consideration regarding the correlation between casting aspects and the microstructure aspects[1].

METHODS: We were casting some samples from cobalt-chromium dental alloys into similar shapes. The researches have been made on cobalt-chromium alloy which are the following nominal composition: Co 63%, Cr 28%, Mo 6%, and 1.5%, Mn <1.5%, Zr<1.5%, Ti<1.5%., without: Be, Cd, Ga and Pb.

The metallographic samples taken from the casting profile have been submitted to the following tests: quantitative optical microscopy (inclusions study), qualitative (metallographic analyses) and scanning electron microscopy coupled with EDS spectrometry. In order to be prepared for optical microscopy examination, the samples were cut, polish, immerse, and dry polish and electrochemical attack with 90 ml water and 10 ml hydrochloric acid and maintaining at 5-10 V for 1-2 minutes. For finding about the nature of our inclusions, we used the scanning electron microscopy and we study the microstructure morphology of some inclusions[2].

RESULTS: The results of the optical microscopy are presented in figure 1. According this, the alloys fit the international standards. Qualitative analysis relived that the alloy has a dendritically structure.

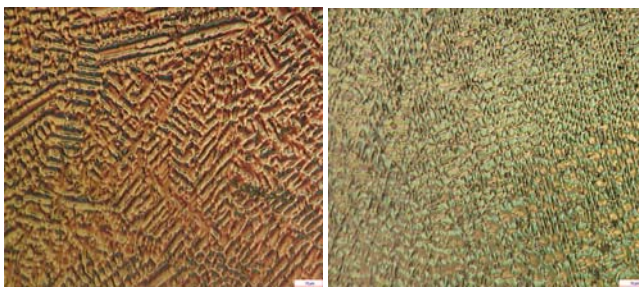

Fig. 1: The optical microscopy images for the Co-Cr samples

Over the surfaces there has been performed EDS quantitative analysis of the composition and also analyses concerning the distribution of the elements on inclusions. The results are presented in figure 2.

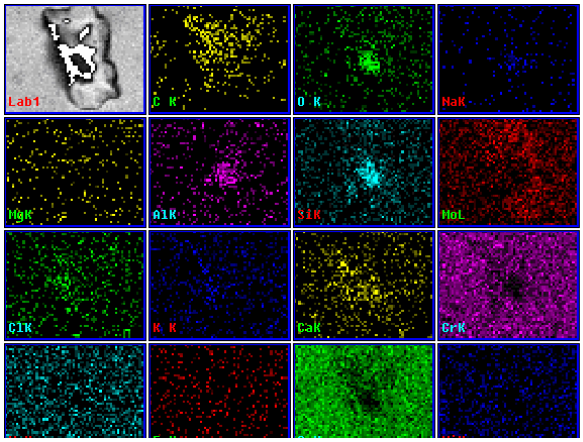

Fig. 2: The scanning electron microscopy of the inclusion and the distribution of the elements on inclusion

We find some non-metallic inclusions, according to the distribution of the elements obtained by EDS quantitative analyses, probably from shapes.

DISCUSSION & CONCLUSIONS: By optical microscopy more structural aspects may be put in evidence, like the presence of carbides with discontinuous precipitation in metallic matrix or the dendritic structure, but better characterization is possible using the scanning electron microscopy. Freedom from non-metallic inclusions is a critical aspect of the castability of the cobalt-chromium dental alloys. In order to perform a better dental application by casting, the cobalt-chromium alloy must have a homogenous and dendritically structure, without inclusions, possible when we make a correlation between microstructure of the alloys and casting technology.

REFERENCES: [1] Saldivar-Garcia AJ, Lopez HF. (2005) *Microstructural effects on the wear resistance of wrought and as-cast Co-Cr-Mo-C implant alloys,* J Biomed Mater Res A. 2005 Aug 1;74(2):269-74. [2] Backovic N, Stamenkovic D. (1982) *The influence of different casting conditions on the microstructure of Co-Cr-Mo alloy,* Stomatol Glas Srb. May-Jul;29(3):183-93. [3] Morris HF. (1990) *Properties of cobalt-chromium metal ceramic alloys after heat treatment,*J Prosthet Dent. Apr;63(4):426-33.

A method for measuring the pulp chamber temperature during light curing

M. Rominu[1], C. Sinescu [1], D. Dodenciu[1], M. Negrutiu[1], A. Kigyosi[1]

[1] *University of Medicine and Pharmacy "Victor Babes" Timisoara, Romania*

INTRODUCTION: The study has as main purpose the description of a method for measuring the pulp chamber temperature during light curing.

METHODS: A class I cavity was prepared in an extracted mandible molar, leaving a dentin layer of 1 mm thick between the pulp chamber and the proximal cavity wall. The measurement of the temperature variations in the pulp chamber (starting with 37+/-0,1^{0}C) [1] was performed with a thermistor inserted in the pulp chamber during polymerization. Another thermistor was inserted in each filling to measure the variation of the temperature in the filling before, during and after the curing (Fig. 2). A 2 mm composite resin (the same in each sample) layer [2] was applied into the cavity and light cured. For the reproducibility process a mark was made on the tooth cavity walls in order to maintain the 2mm composite layer. No etching and bonding materials were used. Taking the filling out was done by high speed drilling in permanent cooling and sharp instruments for leaving a 1 mm thick dentin layer between the pulp chamber and the bottom of the cavity. The curing used units were: halogen unit (Degulux, Degussa), LED (Bluphase C5, Vivadent and MiniLed, DeTrey Dentsply) and plasma unit (Apollo 95E, DMDS). Light curing took place for 20 seconds for halogen and LED units and 6 seconds for plasma unit.

RESULTS: The results of this study are the mediated values of temperature variation recorded in the pulp chamber and in the composite filling during and after curing, untill these variations tend to disappear. The maximum mediated temperature value variation was recorded with the halogen unit (4,2 ^{0}C), higher than for the LED curing (3,0^{0}C), and with plasma unit (1,2^{0}C).

Fig.1. The measurement stand used in this study to measure the pulp chamber temperature.

The main observation is related to the temperature variation values.

The mediated values obtained from the thermistor, one inserted in fillings and the other one inserted in pulp chamber, show that the temperature is also raising in both locations, after the curing light unit was stopped.

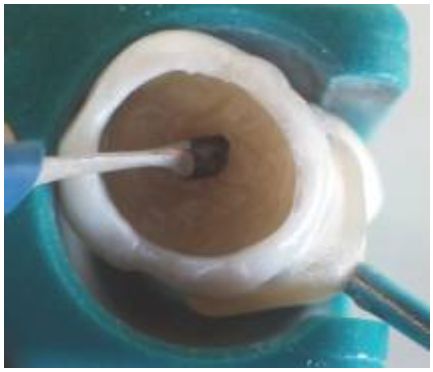

Fig. 2. The thermistor inserted in the filling to measure the variation of the temperature in the composite filling.

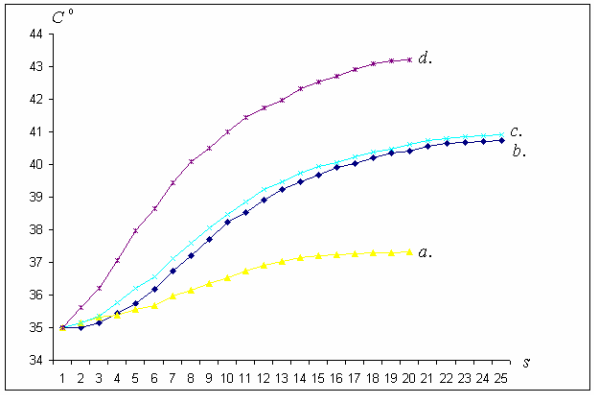

Fig. 3. The temperature variation in the composite filling during and after the curing.

DISCUSSION & CONCLUSIONS: The pulp chamber temperature varies with the type of the light unit used (maximum for halogen curing unit, moderate for LED and minimum for the plasma curing unit) and proportionally with the caloric capacity of the composite material used for filling. Further investigations should be focused in this direction.

REFERENCES: [1] A. Lindberg, A. Peutzfeldt, van J.W. Dijken (2005) *Clin Oral Investig* **9:**71–6.

[2]A. Peutzfeldt, E. Asmussen (2005) *J Dent Res* **84**:659–62.

THE INFLUENCE OF SILANES ON MICROLEAKAGE IN CLASS II COMPOSITE FILLED-CAVITIES

M. Rominu [1], Z. Florita [1], C. Haiduc [1], R.Rominu [1], M. Negrutiu[1], A. Kigyosi [1]

[1] *University of Medicine and Pharmacy "Victor Babes" Timisoara, Romania*

INTRODUCTION: In clinical practice, several types of tooth-colored materials can be used for restoration of class II cavities. Tooth colored restoratives including composites are subjected to marginal leakage [1]. Thermally induced stresses may lead to gap formation and, consecutively, microleakage as a result of mismatch of the coefficients of thermal expansion between the restorative material and the hard dental tissues [2, 3]. The purpose of this study was to investigate to what extent the use of silanes as chemical adhesion promoters influences microleakage in class II cavities restored with a composite resin (Filtek Supreme 3M ESPE).

METHODS: In this study, 30 crack-free and noncarious erupted mandibular third molars were used. A standardized mesial class II cavity (bucco-lingual width 3 mm, occluso-gingival width depending on the tooth and a depth of 2mm) was prepared on each tooth using a regular grit fissure diamond bur. The gingival margin was located approximately 1 mm below the cemento-enamel junction. All teeth were then randomly distributed into three groups, each containing ten teeth. The prepared cavities were restored as follows:

Group 1 – total acid etch (Scotchbond Etchant Phosphoric Acid), Vitremer Primer application (3M ESPE) and Filtek Supreme (dentin A3 shade, 3M ESPE)

Group 2 - total acid etch (Scotchbond Etchant Phosphoric Acid), adhesive application (Adper Single Bond**,** 3M ESPE) and Filtek Supreme (dentin A3 shade, 3M ESPE)

Group 3 - total acid etch (Scotchbond Etchant Phosphoric Acid), application of silane solution (Monobond S, Schaan, Vivadent, Liechtenstein), Adper Single Bond and Filtek Supreme. The silane solution was applied in ample amounts on the gingival margin, left undisturbed 60 seconds, followed by a gentle air dry. Before the application of the adhesive, all surfaces were left moist.

The specimens were stored in distilled water (37°C) for seven days then subjected to 1000 thermocycles between 5 and 55°C with a dwell time of 25 seconds in each bath (transit time 5 seconds). All specimens were then immersed for 24 hours in 2% basic fuchsin with their roots pointing upwards. In this position, the level of dye was 1 mm above the gingival margins of the preparations. Using this technique, dye penetration through improper insulated root areas was avoided. The teeth were sectioned through the middle of the fillings with a water cooled fine grit diamond disc, following a mesial-distal plane. The sections were examined at the gingival interfaces with an optical microscope (model FT MIC 2665, Euromex, Arnhem, Netherlands) at 40X and 100X magnifications. The microleakage scores were chosen as follows: 0 - no dye penetration; 1 - dye penetration up to 1/2 of the cavity depth; 2 - dye penetration to the full depth of the cavity wall (not including the axial wall); 3 - dye penetration along the axial wall.

RESULTS: Microleakage was found in each experimental group. Statistically significant differences were found among the groups (Kruskal-Wallis test, α=0.05, P=0.012). The Mann-Whitney U test revealed statistically significant differences among groups 1-3 (α=0.01, P=0.007) and 2-3 (α=0.05, P=0.033), respectively. No significant differences were found among groups 1-2 (α=0.05, P=0.194).

DISCUSSION & CONCLUSIONS: Because microleakage at the gingival interfaces (dentin/cementum) of class II composite direct restorations nearly always occurs, the efficiency of the adhesive systems to hybridize the cementum layer must be questioned. In this study, the role of silane application in reducing microleakage at the dentin/cementum interface might be explained by its ability in producing chemical bonds with the substrate. Within the limitations of this study it can be concluded that the additional silane treatment of the acid etched gingival margins significantly reduces microleakage in class II composite-filled cavities. Future studies must investigate (1) the chemical mechanism of silane bonding to dentin (2) the ultramorphology of the adhesive/dentin interface and (3) the effects of silane solution on the pulp.

REFERENCES: [1]B.M.Owens (2003), *J. Contemp. Dent. Pract*. **15**:1-9. [2]A. Versluis, W.H. Douglas and R.L. Sakaguchi (1996), *Dent. Mater.* **12**:290-294. [3]K.J. Rossomando and S.L. Wendt Jr. (1995), *Dent. Mater.* **11**: 47-51.

Adhesion formation in response to some biodegradable structures used in mesh repair of abdominal wall hernia

Iulian Antoniac[1], M.Sajin[2], F.Miculescu[1], P.Antoniac[1], M.Ciurea[3]

[1] *University Politehnica of Bucharest.* [2] *Emergency Universitary Hospital Bucharest.*
[3] *University of Medicine and Pharmacy "C.Davila" Bucharest, Romania.*

INTRODUCTION: Most hernia repairs performed today involves the placement of some prosthetic mesh made from different biomaterials. An ideal prosthetic mesh should be chemically inert, non-carcinogenic, and capable of resisting mechanical strain and resist bursting by the maximum forces created by the intra-abdominal pressure. It should allow tissue ingrowth within it resulting in normal pattern of tissue healing and repair without inciting adhesion formation if placed intra-abdominally. The tissue fluids should not physically modify it or incite inflammatory, foreign body or allergic reaction and it should resist infection [l-2]. Many prosthetic materials are used, including polypropylene (PP), expanded polytetrafluoroethylene (ePTFE), polyester and composite (coated with collagen).

METHODS: The purpose of this study was to investigate the adhesion formation in response to some biodegradable structures used in mesh repair of abdominal wall hernia, and to evaluate host tissue response to the prosthetic biomaterials. Some fragments from three type of abdominal mesh made from different biomaterials (polypropylene, polyester and composite polyester-collagen) was excised during surgery from the patients with abdominal hernia.

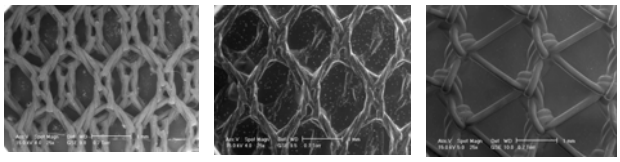

Fig. 1: Scanning electron microscopy of the mesh used in clinical study: Polyester meshes (left), polyester-collagen meshes (centre) vs. polypropylene mesh (right).

The prosthetic biomaterials were excised en bloc with tissue for histological and scanning electron microscopy evaluation.

RESULTS: The results of the histological evaluation are presents in figure 2. The polypropylene and polyester-collagen mesh was very well integrated in the connective tissue, but in the case of polyester mesh was observed the presence of inflammatory elements. We try to use different coloration techniques in order to reveal much better the tissue reaction to different prosthetic materials.

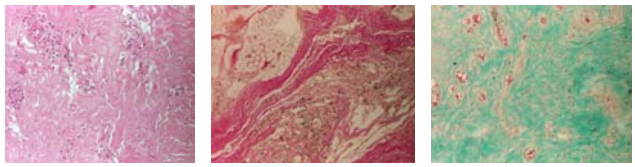

Fig. 2: Histological results - different coloration techniques: Haematoxylin–eozine (left), van Gieson (centre) vs.Tricromic Masson (right)

In order to establish the biodegradability rate of the structures and the adhesion formation we evaluate the same blocs with scanning electron microscopy (figure3).

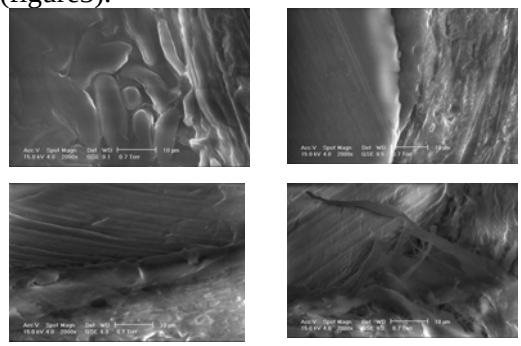

Fig. 3: Scanning electron microscopy of the blocs (tissue-biomaterials interaction aspects).

DISCUSSION & CONCLUSIONS: The combination of prosthetic biomaterials with collagen to form various composite meshes will provide a better biointegration of the mesh in the surrounding tissue. Some different coloration technique used in histological evaluation and scanning electron microscopy appear as a valuable method in order to establish the biodegradability degree of the biodegradable structures used for abdominal mesh.

REFERENCES: [1]W.Vrijland, J.Jeekel (2003) *Prosthetic Mesh Repair Should Be Used for any Defect in the Abdominal Wall.* Curr.Med.Res.Opin. 19:1

ACKNOWLEDGEMENTS: The experimental research was effectuated in the frame of the national research project MEBIOS, financed by the Romanian Research Program CEEX/VIASAN.

Thermic Treatments For Some Welded CoCrMo Alloys Used In Removable Partial Dentures Tehnology

C. Bortun, S. Porojan, L. Sandu, M. Iacob, B. Ghiban

„Victor Babes" University of Medicine and Pharmacy, Timisoara, Romania
University School of Dentistry, Specialization of Dental Technology

INTRODUCTION: Metallic alloys welding (laser welding and microplasma welding) in removable partial dentures technology was studied since 1990 [1,2,3.]. Thermal treatments tend to improve alloys and weldings quality.

METHODS: : There were used three alloys: WIRONIT (Bego), „C" alloy (Vaskut Kohaszati-KFT), HERAENIUM CE (Heraeus-Kulzer), which were casted in plate shape in charges. They were welded with Microplasma Welder (Schutz Dental) and then thermal treated using the same parameters (Fig.1).

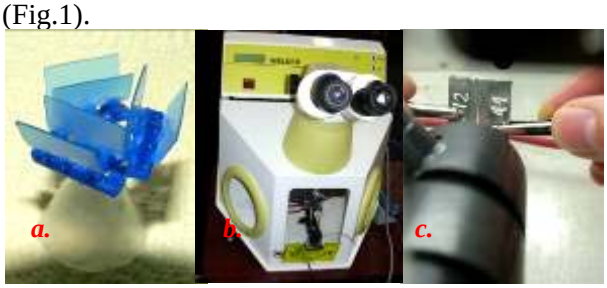

Fig.1: a one wax pattren charge; b. Welder Schutz Dental, c.casted plates welding

RESULTS: 850ºC and 950ºC thermal treatments induced an increasing of Vickers hardness of welded areas, and fragility of the characteristic areas (BM, HAZ, WM). 1050º C temperature was benefit, the hardness and fragility were reduced (table 1)

Table 1 Welding after thermal treatment - Vickers hardness analyses

HERAENIUM CE (Heraeus Kulzer) Alloy WIROVEST investment material				
No.	Test areas	HV5Hardness		
		Welding after thermal treatments		
		850ºC 6.1 + 6.2	950ºC 6.3. + 6.4	1050ºC 6.5 + 6.6
1	BM_6	371	336	371
2	HAZ_1	412	362	349
3	WM	386	473	362
4	HAZ_2	401	345	345
5	BM_2	391	367	376
WIRONIT(Bego) Alloy WIROVEST investment material				
No.	Test areas	HV5Hardness		
		Welding after thermal treatments		
		850ºC/1h 2.1 + 2.2	950ºC/1h 2.3. + 2.4	1050ºC/1h 2.5 + 2.6
1	BM_1	362	349	391
2	HAZ_1	418	447	429
3	WM	502	396	412
4	HAZ_2	423	418	401
5	BM_2	381	371	367

"C"(Vaskut Kohaszati KFT) Alloy WIROVEST investment material				
No.	Test areas	HV5Hardness		
		Welding after thermal treatments		
		850ºC/1h 4.1 + 4.2	950ºC/1h 4.3. + 4.4	1050ºC/1h 4.5 + 4.6
1	BM4	462	418	345
2	HAZ_1	401	401	423
3	WM	447	460	401
4	HAZ_2	412	412	396
5	BM_2	460	376	371

After electropolishing thermal treated weldings hardness parameters indicated a small growth and therefore a fragilization of welded characteristic areas (BM, HAZ, WM) appeared. Microscopic structural analyses noticed welding defects, and some cracks in base materials (Fig.2).

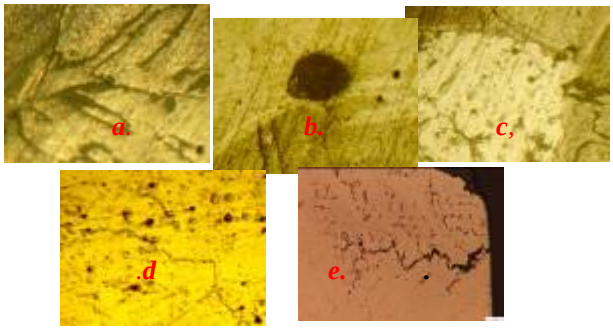

Fig. 2. Welding structural analyses: a. welding, b. welding defect, c. HAZ, d,. base material cracks

DISCUSSION & CONCLUSIONS:
The best behavior to thermal treatment and welding had HERAENIUM CE alloy, the others needed some cooling precautions, possible another thermal treatment at 1050-1150ºC. Hardness quality conditions which guarantees prosthetic pieces durability are between 300 HV and 410 HV.

REFERENCES: [1]C. Bertrand et al., 2004: *Optimization of operator and physical parameters for laser welding of dental materials.* BDJ 196, 413. [2]B.Ghiban et al. 2007: *Structural features in cobalt based alloys for dental applications*, Bull. Transilvania Univ. Brasov, vol.II:80-86. [3]Wang RR et al. 1998.: *Thermal modeling of laser welding for titanium dental restorations.* J Prosthet Dent. Mar; 79(3):335-41

ACKNOWLEDGEMENTS: This study was supported by the CNCSIS Grant, no.744/2006, from the Ministry of Education and Research of Romania

Electrospinning of Drug Loaded Poly(ε-caprolactone) Nanofibers: In Vivo Evaluation of Novel Degradable Small-sized Vascular Grafts

B. Nottelet[1], D. Mandracchia[1], E. Pektok[2], B. Walpoth[2], R. Gurny[1], M.Möller[1]*

[1]Department of Pharmaceutics and Biopharmaceutics, School of Pharmaceutical Sciences, University of Geneva, University of Lausanne, Geneva, Switzerland. [2]Cardiovascular Research, Service of Cardiovascular Surgery, University Hospital of Geneva, Geneva, Switzerland

INTRODUCTION: Most ischaemic diseases like atherosclerosis require a revascularisation procedure. They can be treated by bypass surgery with autologous or homologous graft material but such material is not always available nor suitable[1,2]. For this reason *in vitro* tissue engineering and biostable synthetic prostheses have been proposed, and latter are widely used. However these solutions are not fully satisfactory, especially when replacing small blood vessels (Ø<6mm) where acute thrombosis and intimal hyperplasia occur[3]. To overcome the drawback of permanent residence of the grafts in the body we prepared biodegradable small vascular grafts composed of poly(ε-caprolactone) (PCL) nanofibers containing an anti-inflammatory drug. The simultaneous degradation of the graft and controlled localized drug release should favour the *in vivo* natural blood vessel reconstruction.

METHODS: PCL solutions (7.5-15%,w:v) containing dexamethasone (0-10%,w:w) were prepared in chloroform/ethanol mixtures. The solutions were electrospun (1kV/cm) and the formed nanofibers collected onto a 2mm diameter mandrel. After drying and sterilization of the grafts, their mechanical and morphological properties have been evaluated. Preliminary *in vitro* drug release studies as well as *in vivo* implantation in rats have been carried out and are still ongoing.

RESULTS: A factorial design approach was used to prepare 2mm diameter grafts having a controlled morphology mimicking the extracellular matrix and mechanical properties similar to those of native vessels. Whatever the drug loading, controlled fiber sizes are obtained with mean diameters in the range of 500nm to 2000nm, which are suitable for the use in vascular grafts. As previously described[4], fiber diameter increases with PCL concentration while the opposite occurs for beads. In fact, beads were only found for 7.5% and 9% solutions, while no beads were detected for the 12% and 15% solutions (Fig.1). Furthermore, the mechanical properties were suitable for almost all the non loaded grafts with maximum stress values above 2MPa, value found for natural blood vessels, and maximum strain values around 250% for the 7.5 and 9% solutions and 3-fold higher values for the 12 and 15% solutions. Dexamethasone loaded grafts showed even better mechanical properties.

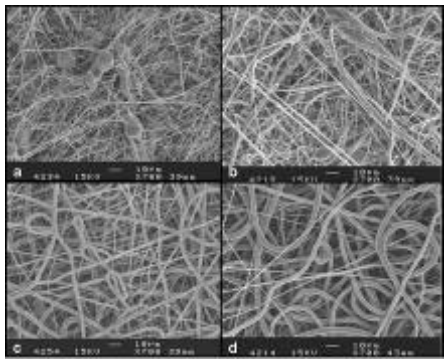

Fig.1: Influence of PCL solution concentration on fibers morphology with a) 7.5 %, b) 9%, c) 12%, and d) 15% .

Preliminary *in vivo* studies in rats followed up by angiography and histological studies have shown good patency (Fig.2a), the formation of an intima without hyperplasia (Fig.2b) and diffusion of cells without inflammation. Long term studies are under progress for *in vivo* functionality and degradability evaluations.

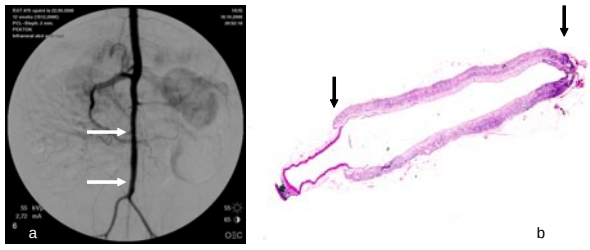

Fig.2: a) angiography and b) histological cross section of a 12 weeks implanted PCL vascular graft in rat.

DISCUSSION & CONCLUSIONS: 2mm diameter biodegradable vascular grafts made of PCL and containing dexamethasone have been successfully prepared and implanted in rats and led to promising results.

REFERENCES: [1] R. Emery (1996) *Ann Thorac Surg* **62**:691-95. [2] K. Brockbank (1992) *J Cardiac Surg* **7**:170.76. [3] O. Teebken (2002) *Eur J Vasc Endovasc* **23**:475-85. [4] N. Bolgen (2005) *J Biomat Sci-Polym E* **16**:1537-55.

*Michael.Moeller@pharm.unige.ch

Corrosion resistance of the biocompatible nitride and carbide thin films

C.M.Cotrut[1], A. Vladescu[2], I. Antoniac[1], A.Kiss[2], R. Zamfir[1], C.N.Zoita[2], M.Braic[2], V.Braic[2]

[1]University Politehnica of Bucharest, Romania [2] National Institute for Optoelectronics-Tehnoprof Research Centre, Romania

INTRODUCTION: In the last few years considerable research effort was directed to deposition of biocompatible thin films in order to increase the wear and corrosion resistance and life of various implants and prostheses [1]. In this paper, synthesis and characterization of TiN, TiC, Ti(C,N), ZrN and (Ti,Zr)N films prepared under different deposition conditions by a cathodic arc system are presented.

METHODS: The thin films were deposited using cathodic arc technique using Ti and Zr cathode targets [2]. These coatings were prepared in a reactive atmosphere of N_2 and CH_4+N_2, respectively. Hard coatings deposition was performed on Si and stainless steel substrates. The overall thickness of all coatings was approx. 2 μm. Elemental composition was investigated by Auger electron spectroscopy (AES). Phase composition and texture were determined by X-ray diffraction. Microhardness measurements were performed using a microhardness tester at 15 g load. Scratch tests under standard conditions were undertaken to determine the coating adhesion. The electrochemical test was used in order to determinate the corrosion resistance by measuring the corrosion current and the critical current for passivation. The test consisted of potentiodynamic polarization from -1100 to +1100 mV with a scan speed of 20 mV/s of the coated samples in artificial physiological solution.

RESULTS: The AES analysis showed that the layers are formed by almost stoichiometric layers (N/Ti≈N/Zr≈C/Ti≈(N+C)/Ti≈N/(Ti+Zr)≈1). For the (Ti,Zr)N film, Zr content is significantly higher that Ti content (Ti/Zr= 0.45). All types of coatings exhibited a strong (111) preferred orientation. For the (Ti,Zr)N coating, the diffraction lines were located nearby the positions of the lines found for the ZrN film, but with a slight shift ($0.5\text{-}0.7^0$) towards higher Bragg angles. This shows, as it was evidenced by the analysis of the elemental composition, that the Zr concentration in the film is substantially higher than that of Ti. One may conclude that the investigated layer crystallized in a face centered cubic ZrN lattice with reduced lattice parameters. Microhardness HV values were in the range 22÷26 GPa - TiN, 26÷28 GPa - TiC, 28÷35 GPa - TiCN, 25÷28 GPa – ZrN and 27÷34 GPa - TiZrN. A good adhesion of all films was found, critical loads of 40 – 57 N being measured. The best corrosion resistance was measured for the TiCN and TiZrN coatings followed by ZrN, TiC and TiN. It can be seen that the coatings improved the corrosion resistance of the uncoated specimens, by decreasing value of the critical corrosion current, as previously reported for some transition metal nitride and carbide coatings [3,4].

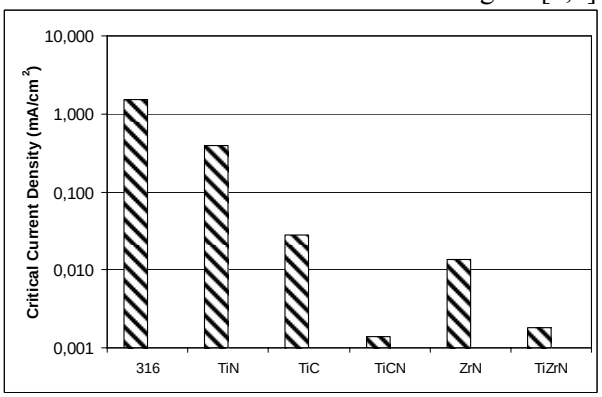

Fig. 1: Critical current densities of the coatings and substrate.

DISCUSSION & CONCLUSIONS: Coatings of transition metal nitrides (TiN, ZrN, TiZrN) and carbides (TiC, TiCN) were deposited on 316L substrates in order to enhance the corrosion resistance in artificial physiological solution of austenitic stainless steels. All coatings have shown the highest corrosion protection, exhibiting the lowest value of the critical corrosion current. Since the TiCN and TiZrN coatings were found to have the highest microhardness and adhesion and also a good corrosion behavior, these types of films would be an appropriate solution to enhance the performance of the stainless steel implants.

REFERENCES: [1] S. Black, (1999) *Biological performance of materials: fundamental of biocompatibility*, 3rd edition, Ed. Dekker, New York. [2] M. Braic, M. Balaceanu, V. Braic, A. Vladescu, G. Pavelescu, M. Albulescu (2005) Surf.Coat.Technol. **200**, 1014-1017. [3] M. Ürgen, A.F. Çakir (1997) Surf.Coat.Technol. **96**, 236-44. [4] E. Kelesoglu, C. Mitterer, M. Ürgen (2002) Surf. Coat. Technol.**160**, 82-86.

Acknoledgements: The work presented in this paper was supported by CEEX Program, under Osteosurf 235/2006 project.

Measuring cell adhesion forces as a function of the cell cycle by force spectroscopy

G. Weder[1], M. Giazzon[1], J. Polesel-Maris[1], A. Meister[1], M. Liley[1], H. Heinzelmann[1]

[1] *Centre Suisse d'Electronique et de Microtechnique, Jaquet-Droz 1, 2002 Neuchâtel, Switzerland.*

INTRODUCTION: The study of cell-surface interactions is important for several different applications, notably that of medical implants. In the context of bone implants, CSEM is studying the effect of surface structure on the behaviour of osteoblasts. While the effects of surfaces on cell proliferation, alignment, structure and growth are accessible via traditional microscopy and labelling techniques, the determination of cell adhesion remains a major challenge. In the European project Newbone, CSEM will study osteosarcoma (SaOs-2) cell adhesion forces on structured surfaces of fibre-reinforced composite-based non-metallic bone implant materials. Atomic force microscopy, and particularly force spectroscopy will be used to directly measure the adhesion of the cell on the surface.

The adhesion of cells on surfaces depends very strongly on the phase of the cell cycle (G_0, G_1, S, G_2 or M). In order to obtain meaningful results, it is necessary to study cell/surface adhesion for each phase separately. For this reason, initial work has focussed on obtaining synchronised osteoblasts to compare cell adhesion by force spectroscopy in the different phases of the cell cycle.

METHODS: The Saos-2 cell line was from the ATCC collection (LGC Promochem, France) and cultured in modified McCoy's 5A Medium with L-glutamine supplemented with 10% heat-inactivated FCS. Saos-2 cells were synchronized using a protocol adapted from Galgano *et al.* [1] with the plant amino acid mimosine as a G_0/G_1 synchronizing agent and with nocodazole as a G_2/M synchronizing agent. Saos-2 cells were seeded into tissue culture flasks 24 hours before beginning the presynchronization with FCS-free medium during 10 hours. Osteoblasts were exposed to 0.4mM of mimosine or to 0.6µg/ml of nocodazole for 48 hours. The S phase is reached by releasing cells from mimosine arrest by removing mimosine-containing medium and adding complete growth medium for about 18 hours. DNA content was measured using an EPICS® XL-MCL™ flow cytometer (BeckmanCoulter, Germany) with propidium iodide labelling.

RESULTS: The Saos-2 cells show a synchronization of 86% in the G_0/G_1 phase and of 70% in the G_2/M phase. A broader peak is obtained on S phase synchronization reflecting the dissipation of cell synchronization 18 hours after mimosine release.

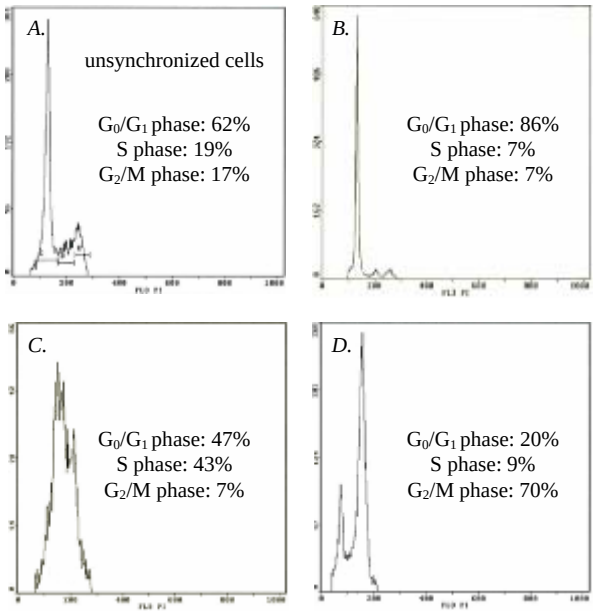

Fig. 1: Human osteoblasts (Saos-2) synchronized at 3 points of the cell cycle by cell cycle inhibitors: mimosine for G_0/G_1 (B) and S with mimosine release (C) and nocodazole for G_2/M (D). Comparison with unsynchronized cells (A).

DISCUSSION & CONCLUSIONS: Good synchronization has been obtained in the G_0/G_1 and G_2/M phases. However, we need still to optimize the releasing time after a reversible mimosine arrest to reach S phase. These will constitute the 3 checkpoints in the cell cycle to perform cell adhesion measurements by force spectroscopy via atomic force microscopy and allow an analysis of the influence of surface structure on cell adhesion.

REFERENCES: [1]P. J. Galgano et al. (2006) *CSH Protocols* doi:10.1101/pdb.prot4488.

ACKNOWLEDGEMENTS: We thank Dr Amira Sarraj of the *Laboratoire du Service régional Neuchâtelois et Jurassien de Transfusion Sanguine (SRNJTS)* in La Chaux-de-Fonds (CH) for use of their flow cytometer.

European Cells and Materials Vol. 13. Suppl. 3, 2007 (page 36) ISSN 1473-2262

Interconnected Porous Scaffolds for Bone Augmentation

F. Fierz[1], F. Beckmann[2], B. Leukers[3], S. Irsen[3], M. Huser[4], A. Andronache[4], and B. Müller[1]

[1] Biomaterials Science Center, University of Basel, Switzerland. [2] GKSS-Research Center Geesthacht, Germany. [3] Caesar Research Center, Bonn, Germany. [4] Computer Vision Laboratory, ETH Zürich, Switzerland.

INTRODUCTION: Tissue engineering based on interconnected porous ceramic scaffolds and autologous cells belongs to promising approaches for filling bone defects. The scaffold's morphology including 3D porosity and interconnectivity is a key issue for optimizing the osseointegration of the generated implants. Tomograms obtained by synchrotron radiation-based micro computed tomography (SRμCT) are the basis for the 3D characterization of the scaffolds on the micrometer scale using sophisticated tools such as distance mapping, component labeling, dilatation/erosion, and image registration.

METHODS: Hydroxyapatite scaffolds in three different designs made layer-by-layer were fabricated using rapid prototyping and sintering.[1]

SRμCT measurements were performed at the beamline W 2 (HASYLAB at DESY, Hamburg, Germany), operated by GKSS, with the pixel size of 3.7 μm using the photon energy of 30 keV.

For the data analysis, software packages were developed for rigid registration with 9 parameters (3 rotation, 3 translation, 3 scaling), for 2D and 3D distance mapping, for component labeling to determine the pores' interconnectivity, and for masking to quantify the scaffold's quality.

RESULTS: The mean distance to material derived from the 2D distance mapping (Fig. 1) is between 133 and 148 μm and depends on the selected design. The 3D analysis provided values without significant spreading (98 - 100 μm).

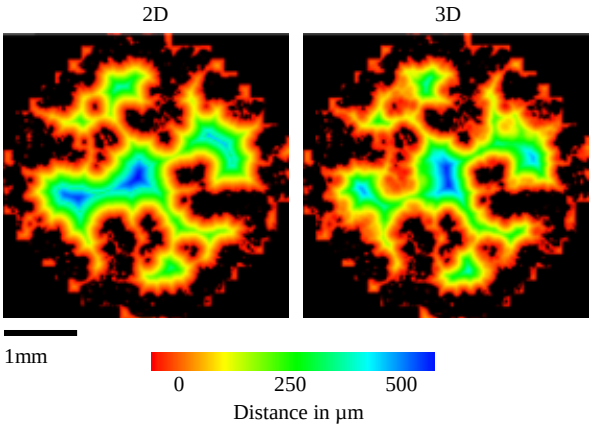

Fig. 1: 2D (left) and 3D (right) distance map: black indicates scaffold material.

The component labeling gives rise to a perfectly interconnected channel network in the scaffold. The major air component covers (99.53 ± 0.09)%. By the definition of a smallest diameter that cells can pass, we are able to determine the parts of the cavity accessible for the cells by migration.

The 3D image registration of the design with the tomograms of sintered scaffolds yields the printing quality (Fig. 2). It allows calculating the shrinking in the three orthogonal directions. The shrinking is almost isotropic and corresponds to (73 ± 2)%.

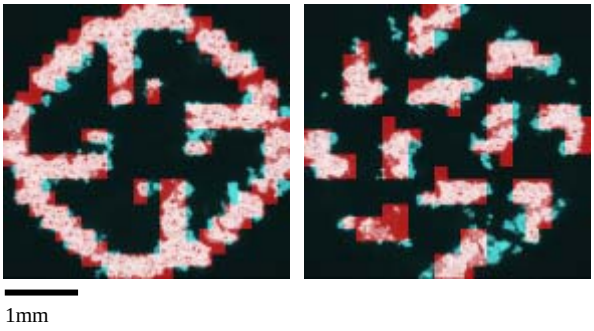

Fig. 2: Image registration of design (mask) and tomogram of scaffold. The mask is red-colored, material outside the mask blue and material printed inside the mask white.

DISCUSSION & CONCLUSIONS: The digital, 3D data nondestructively obtained by SRμCT are the perfect basis for the visualization and quantification of the scaffold morphology. The application of standard software, however, is difficult because of the huge data size in the range of GB and hence specific code was developed. The distance mapping clearly demonstrates that the 2D analysis overestimates the mean distance to the material by 30 to 50%. Component labeling together with appropriately selected minimal diameters for cell migration allows visualizing the parts of the scaffold that are accessible by biological cells seeded. 3D registration algorithms are shown to allow for the precise measurement of the shrinking as the result of the sintering process and for the detailed evaluation of the scaffolds morphology with respect to the planned design.

REFERENCE: [1]S. Irsen et al (2006) *Material-wissenschaft und Werkstofftechnik* **37**:533-537.

ACKNOWLEDGEMENT: HASYLAB at DESY (Proposal I-05-028), Hamburg, Germany.

Nanostructured Ceramic Coatings for Drug Delivery

K. Dittmar[1], A. Tourvielle[2], H. Hofmann[1], C. Lowe[2]

[1] *Laboratory of Powder Technology, EPF Lausanne, Lausanne, Switzerland.*

[2] *Debiotech SA, Lausanne, Switzerland.*

INTRODUCTION: Medical implants delivering drugs are often used to ensure efficient medication at body sites where systemic administration is insufficient or could be harmful. The combination of a drug delivery coating on a mechanically supporting substrate is a beneficial concept for implants exposed to loads, e.g. stents or orthopaedic implants. Many of the commercially available coated stent implants are designed to release a drug locally and with a predefined rate out of a polymer matrix. These polymers are either biodegradable, bio-erodible or inert. In spite of their successful drug release capability, they have often failed in regards to biocompatibility, long-term chemical and mechanical stability [1].

This project drives to develop a thin layered ceramic based coating providing local drug delivery. It should feature a high level of biocompatibility, wear and chemical resistance, adjustable and prolonged drug release.

METHODS: The coating is produced by a multi-step dip coating technique, as shown schematically in Figure 1 [2]. A following burn out of template particles creates the drug reservoirs. The study of the mechanical properties of the coating, the drug loading and release characteristics are under current investigation.

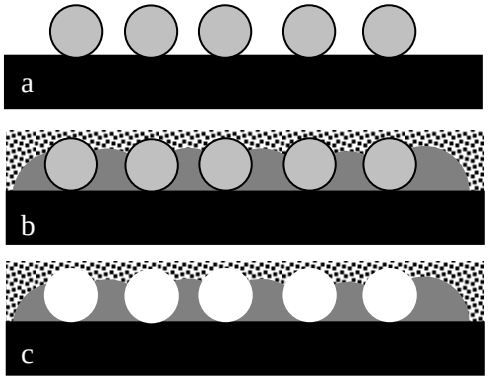

Fig. 1: Manufacturing of the ceramic coating: a: polymeric microbeads deposition; b: enclosure by a ceramic nanoparticle suspension; c: the thermal treatment creates macroporous holes to serve as drug reservoirs.

RESULTS: Structured multilayered TiO_2-films on an electropolished stainless steel substrate have successfully been manufactured (Figure 2). The drug reservoirs in sizes of 1-5 µm can either be open to the external surface or enclosed by an outer ceramic layer. The porosity (micro or meso size) of that film serves as a barrier for the drug diffusion from the reservoirs into the surrounding tissue.

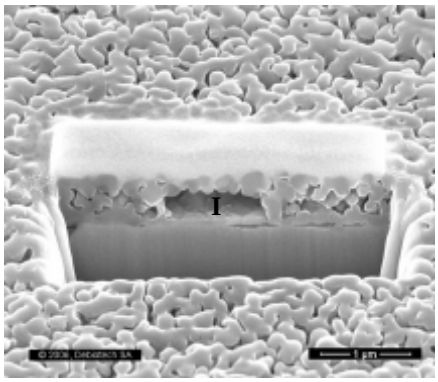

Fig. 2: Ceramic coating with the macropore (I) and a mesoporous ceramic layer on top.

DISCUSSION & CONCLUSIONS: The results obtained up-to-date are very encouraging to apply these ceramic coatings to implantable medical devices such as drug eluting stents. One major challenge lies in the compromise between a thin mechanically stable coating and the drug loading levels needed for the clinical application. Therefore the detailed determination of the coating's mechanical properties, the characterization of the porous structure and its drug loading capacity have to be considered. Drug release testing under physiological conditions will help to establish a drug diffusion model. It integrates the structural parameters of the coating, the colloidal effects, as well as the physico-chemical features of the drug itself. This model aims to transfer the technology of this nano- and microporous coating to multiple implantable medical devices using different drugs.

REFERENCES: [1] R. S. Schwartz, et al (2006) *Advanced Drug Delivery Reviews 58:377-386.* [2] F. Juillerat (2005) *Self-assembled nanostructures prepared by colloidal chemistry, Doctoral Thesis EPFL.*

ACKNOWLEDGEMENTS: Thanks to CTI and Debiotech SA for financing this interesting project.

Microtomography on Biomaterials using the HARWI-2 beamline at DESY

J. Herzen[1], F. Beckmann[1], B. Müller[2], F. Witte[3], T. Donath[1], B. Leukers[4], S. H. Irsen[4], M. Störmer[1], N. Hort[1], A. Schrott-Fischer[5], R. Glueckert[5], and A. Schreyer[1]

[1]GKSS-Research Center, Geesthacht, Germany. [2]Biomaterials Science Center, University of Basel, Switzerland. [3]Laboratory for Biomechanics and Biomaterials, Hannover Medical School, Germany. [4]ceasar research center, Bonn, Germany. [5] ORL University Clinics, Medical University Innsbruck, Austria

INTRODUCTION: The synchrotron radiation beamline HARWI-2 operated by the GKSS-Research Center in cooperation with Deutsches Elektronen-Synchrotron DESY, Hamburg, Germany is designed for materials science experiments using hard X-rays. A fixed-exit monochromator provides a highly intense, monochromatic X-ray beam in the energy range between 15 and 200 keV [1]. This large range of photon energies, the spatial resolution down to 3 µm and the related density resolution are important for microtomographic applications. The advantages of the beamline are demonstrated for absorption contrast tomography on the field of biomaterials.

METHODS & MATERIALS: The homogeneity of the collagen coating of the 3D-printed and collagen-coated scaffolds for bone replacement has been analysed using synchrotron radiation based micro computed tomography (SRµCT) in absorption mode at a photon energy of 30 keV. The collagen coating significantly improves the mechanical stability of the scaffolds [2].

Cortical bone screws were machined from magnesium alloy AZ31 extruded rods. These screws were implanted into hip-bones of sheep and removed from the animals three months later. Afterwards SRµCT was performed at a photon energy of 30 keV to study the corrosion behaviour of the screws.

The cochlear implant consists of 12 electrodes and was inserted into the inner ear of a patient with a sensory neural hearing loss. The electrode stimulates electrically the sensory cells in the cochlea. The implant with surrounding tissue was removed 36 hours after the patient's death and fixated in Karnosky solution. To improve the soft tissue density resolution, the entire specimen was stained with 1% OsO_4. The measurements were performed in absorption contrast mode using the photon energy of 64 keV [4].

RESULTS & CONCLUSIONS: The superior density resolution of the SRµCT at HARWI-2 allows visualizing non-destructively the 3D distribution of collagen coating on bone replacement scaffolds.

The SRµCT enables to describe non-destructively the in-vivo corrosion of engineered cortical magnesium (AZ31) screws in sheep bone and thereby overcomes artefacts associated with the preparation of magnesium materials soluble in water and body fluids [3].

The detailed analysis of the cochlear implant also takes advantage of the microtomography for visualizing non-destructively the temporal bone structures of the inner ear, the position of the electrode array and for characterizing the integration of cochlea implants almost free of any artefacts (Fig.1). In contrast histological techniques that are commonly applied, are accompanied by artefacts caused by the preparation methods, especially for metallic cochlear implants when the electrode array in the embedded tissue specimen block has to be cut.

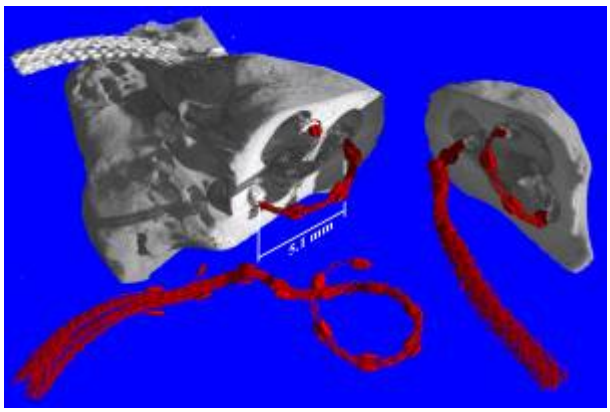

Fig. 1: The metallic cochlea implant consisting of an array of 12 pairs of electrodes and the winding of the human cochlea.

Due to the wide energy range and the superior contrast the SRµCT at HARWI-2 provides non-destructive high quality 3D visualization of a large range of different materials. Even samples with a dimension of several centimetres can be analysed with a very low amount of artefacts.

REFERENCES: [1] F. Beckmann et al. (2006) *SPIE Proceedings* 631810-1-11. [2] S. H. Irsen et al. (2006) *SPIE Proceedings* 631809-1-10. [3] F. Witte et al. (2006) *SPIE Proceedings* 631806-1-9. [4] B. Müller et al. (2006) *DESY Annual Report 2006*, 1291-1292

European Cells and Materials Vol. 13. Suppl. 3, 2007 (page 39) ISSN 1473-2262

Morphology of Osteoblasts Grown on Doped Diamond-Like Carbon Coatings- An Electron Microscopy Study

B. Saldamli[1], G. Thorwarth[2], P. Jürgens[1], C. Hammerl[3], M. Kuhn[3], B. Stritzker[2], R. Sader[4] and C. Leiggener[1]

[1] University Hospital, Basel, Switzerland. [2] Institute for Physics, University of Augsburg, Germany. [3] AxynTeC GmbH, Augsburg, Germany. [4] Oral, Cranio-Maxillofacial & Plastic Facial Surgery, J. W. Goethe University, Frankfurt am Main, Germany.

INTRODUCTION: Diamond-like carbon (DLC) coatings can be produced by several methods, including plasma immersion ion implantation and deposition (PIII&D). PIII&D is a method that allows the uniform coating of objects with complex geometries and the production of surface gradients that are especially important for the adhesion of DLC on metallic substrates. Further, with PIII&D various dopants can be incorporated into the DLC layer to produce variations in the surface physicochemistry and hence to alter the biological response. We studied the effect of Si-, H-, N-, and TiO-doping of DLC on human osteoblast adhesion and morphology.

METHODS: DLC-coatings were deposited on TiAl6V4 substrates with turned surface finish (R_a = 520 nm) by an ECR-based PIII&D process [1]. Five DLC variants were produced: non-doped ("0"), silicon-doped ("Si"), hydrogen-doped ("H"), nitrogen-doped ("N"), and titanium oxide-doped ("TiO") DLC by adding corresponding dopant precursors. They were characterized by elastic recoil detection analysis (ERDA) and Rutherford backscattering (RBS), see Tab. 1. Human osteoblasts were isolated, seeded on the DLC-coated and uncoated TiAl6V4 substrates, and incubated as previously described [2]. After 4 h and 24 h the cultures were washed, fixed in 2% glutaraldehyde, postfixed in 1% OsO_4 and dehydrated in graded series of alcohol and HMDS. The cell morphology was examined with an environmental SEM equipped with a BSE detector for imaging of elemental contrasts.

Table 1. PIII&D precursor gases and resulting composition of the DLC coatings.

DLC type	Precursor gases	Composition (at.%) (ERDA/RBS)
0	Hydrocarbon, Ar	C: 69, H: 30
Si	Hydrocarbon, Ar, HMDS	C: 57, H: 30, Si: 10, N: 3
H	Hydrocarbon, Ar, H_2	C: 60, H: 40
N	Hydrocarbon, Ar, N_2	C: 75, H: 22, N: 3
TiO	Hydrocarbon, Ar, $TiCl_4$, CO_2	C: 40, H: 18, Ti: 19, O: 23

RESULTS: The SEM images revealed similar osteoblast morphology on the DLCs and the TiAl6V4 surfaces for both culture periods. The cells adhered readily on all surfaces after 4 h and exhibited a round shape with discrete cytoplasmic extensions at periphery. After 24 h the osteoblasts switched to the polygonal morphology with prominent cytoplasmic extensions (Fig. 1).

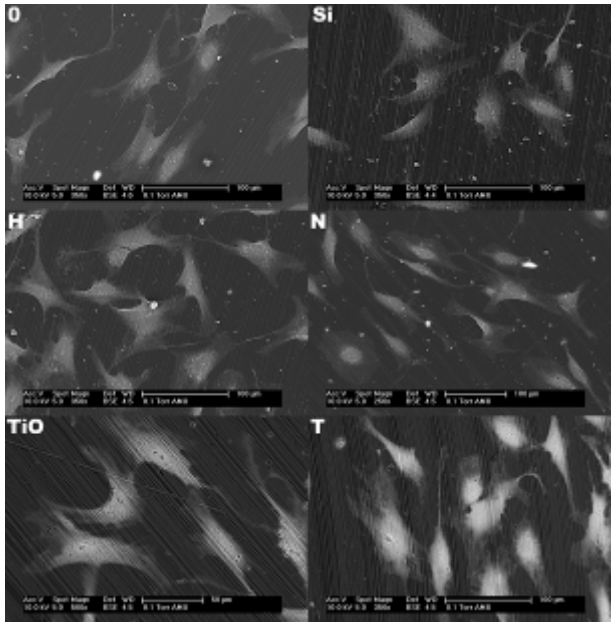

Fig. 1: Osteoblast morphology on the different DLC surfaces: non-doped (0), Si-doped (Si), H-doped (H), N-doped (N), TiO-doped (TiO), in comparison to TiAl6V4 (T) after 24 h in culture.

DISCUSSION & CONCLUSIONS: The successful osteointegration of an implant relies on its ability to support the building of bony tissue on its surface. In order to proliferate and subsequently produce ECM components, osteoblasts need to adhere and spread on the implant surface. Our results show that the selected DLC coatings are favorable for osteoblast adhesion and spreading similar to TiAl6V4.

REFERENCES: [1] G. Thorwarth, C. Hammerl, M. Kuhn, et al (2005) *Surf Coat Technol* **193**:206-212. [2] G. Thorwarth, B. Saldamli, F. Schwarz, et. al (in press) *Plasma Process Polym* DOI: PPAP 200731001 I.R.

ACKNOWLEDGEMENTS: We acknowledge the financial support of the *Bayerische Forschungsstiftung* and the supply of the TiAl6V4 substrates by *Peter Brehm GmbH* (Erlangen, Germany).

European Cells and Materials Vol. 13. Suppl. 3, 2007 (page 40) ISSN 1473-2262

Amphiphilic Copolymers at the Air-Water Interface for the Preparation of Calcium Phosphate Thin Films

O. Casse[1], A. Taubert[2]

[1] *University of Basel, Basel, Switzerland.* [2] *University of Potsdam, Golm, Germany.*

INTRODUCTION: A series of poly(n-butyl acrylate)-block-poly(acrylic acid) in a Langmuir monolayer system is presented as a good template to generate calcium phosphate (CaP) thin films. Those hybrid flexible films offer controlled thickness and organic-inorganic ratio. As fixed horizontal surfaces offer simpler conditions for study and modeling of processes such as charge interaction, complexation and crystal nucleation, when compared to colloids, those films can be considered as a step towards studying the coating of organic nanoparticles.

METHODS: A KSV Langmuir-Blodgett system with moving barriers assigned to surface pressure control and automatic dipping for solid substrates was used to create the films. Subphases consisted of buffered water calcium solutions in a Teflon trough. After the polymer was cast on the water surface from a small volume of a chloroform solution, time was left for the calcium to complex with the acid moieties. The phosphate counter-ion was then added with a syringe at the bottom of the trough through the polymer monolayer.

Optical, transmission/scanning electron and atomic force microscopies were used to characterize the films.

RESULTS: Films were obtained only at basic pH, whereas at low pH the polymer monolayer would keep most of its original elasticity. Organic/inorganic ratio within the films were controlled by 3 parameters: the polymer monolayer stress ("solid" or "liquid" phase of the Langmuir isotherm), the supersaturation of the subphase and the mineralization time. In all cases at basic pH the elastic polymer monolayer was rendered stable over time and compact (unable to extend upon decompression) and brittle when transferred to solid substrates.

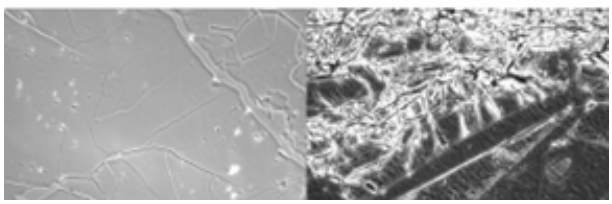

Fig. 1: optical microscopy images of a dried hybrid CaP-polymer film transfered on glass (left: bright field, right: dark field, wrapped film after collapse), witdh 300µm.

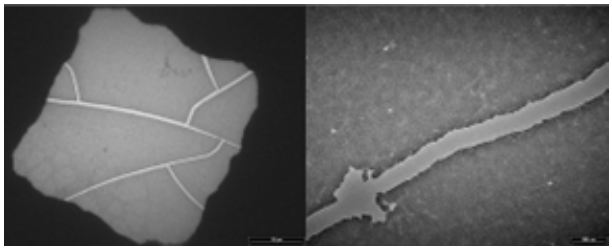

Fig. 2:Transmission electron microscopy images (left width: 60µm, right width: 2µm)

DISCUSSION & CONCLUSIONS: The widescale monolayer homogeneity of the films showed above speak in favour of a mechanism of mineralization where the CaP was nucleated by the polymer carboxylic acid moieties (quick with respect to the further growth of CaP mineral). Other mechanisms including nucleation of CaP in solution before aggregation under the polymer monolayer would result in very inhomogeneous mineral layers in terms of thickness and density, which both the TEM and optical micrographs would reveal.

REFERENCES: [1] E. DiMasi (2002), *Langmuir, Polymer-Controlled Growth Rate of an Amorphous Mineral Film Nucleated at a Fatty Acid Monolayer*, **18**, pp 8902-8909. [2] E. Eghbali, O. Colombani (2006), *Langmuir, Rheology and Phase Behaviour of poly(n-butyl-acrylate)-block-poly(acrylic acid) in aqueous solution,* **22**(10), pp 4766-4776.

ACKNOWLEDGEMENTS: We thank Olivier Colombani (University of Le Mans, France) and Axell Müller (University of Bayreuth, Germany) for providing us with the polymers and characterizing the polymer monolayers, and Sandro Erni (University of Basel, Switzerland) for performing mineralization experiments.

CLINICAL APPLICATIONS OF ^{90}Y GLASS MICROSPHERES IN ONCOLOGY: OPPORTUNITIES AND RISKS

D. T. Eniu[1], Daniela Eniu[2], Ioana Neagoe[3], Ioana Brie[3], Viorica Simon[4], S. Simon[4]

[1] Oncology Institute "Ion Kiricuta", Surgical Department, Cluj-Napoca, Romania; [2] University of Medicine and Pharmacy, Faculty of Pharmacy, Biophysics Department, Cluj-Napoca, Romania; [3] Oncology Institute "Ion Kiricuta", Experimental Research Department, Cluj-Napoca, Romania; [4] Babes-Bolyai University, Faculty of Physics, Cluj-Napoca, Romania.

High-energy and long-range external gamma irradiation often causes the destruction of the healthy tissues it goes through before it reaches, in a weakened state, the malignant one. When the irradiation dose is too high, unwanted irradiation of the surrounding tissues is caused, which is not beneficial either to the body or to the evolution of the malignant tumor. Beta radiation has a short range and is not suitable for external beam irradiation when the malignant tissues are situated deeper inside the body.

The in situ utilization of radiotherapeutic glasses for the irradiation of different tumors was motivated by the fact that the action of radiation in the human body has to be localized very precisely, which supposes as efficient a radiation as possible of the tumor itself with as little effect as possible on the surrounding healthy tissues and organs. In this case the dose administered to the tumor can be much higher (> 10.000 rads = 100 Gy) as compared to the maximum external irradiation limit (recommended to be of 3.000 rads = 30 Gy), which leads to increased irradiation effectiveness.

Radioactive glasses are used as radiation "delivery vehicles". In order for them to be used in radiotherapy, the glasses must: be biocompatible, be insoluble while radioactive and have a high degree of chemical purity. REAS glasses can be activated by neutron bombardment in the last stage, without involving risks or special precautions during the previous stages related to glass microspheres preparation, thus being highly applicable in cancer radiotherapy.

These are used successfully for the treatment of various cancers and tumors. Since response to chemotherapy and external radiotherapy is not so effective and hazardous too, so an alternative to this is internal radiation therapy. These radiolabeled microspheres are very stable and have a proven efficacy in the field of primary as well as metastatic cancers. Radioactive microspheres can be selectively targeted to various tumors without undue radiation to the nontumorous tissues. The radioactive microspheres are injected to halt tumor growth via the blood supply, thereby enabling surgical removal once the tumor size decreases.

Aluminosilicate glasses with rare earth elements are currently applied clinically to the irradiation of diseased kidneys before surgical removal, the irradiation of the synovial membrane in arthritic joints and the irradiation of malignant liver tumors. Currently used treatments for unresectable hepatic cancer require hospitalization, and usually cause side effects that reduce the quality of life for patients. Treatment of hepatic cancer with external beam radiation showed that it is sensitive to radiation but the major drawback is that it cannot be tightly focused on the tumor and it affects a larger area of the body that includes the tumor. The glass microspheres for the treatment of tumors in the liver are infused through a catheter into the hepatic artery. After the treatment, they remain undefined fixed in the liver, without causing any symptom or damage.

The risks the use of the microspheres implies are: acute inflammation of the normal tissue (e.g. hepatitis), run out in the systemic circulation with pneumonitis, bone marrow suppression, gastrointestinal bleeding and pulmonary fibrosis.

Any tissue that is relatively insensitive to small or moderate doses of ionizing radiation and permits the deposition of the microspheres either by blood supply either by surgical implantation, represents a potential candidate for this new form of therapy.

This review provides an outlook to various aspects of radioactive microspheres and their role in the treatment of various cancers.

REFERENCES: [1] Riad Salem , MD , MBA, and Kenneth G. Thurston, MA *Radioembolization with 90Yttrium Microspheres: A State-of-the-Art Brachytherapy Treatment for Primary and Secondary Liver Malignancies* J Vasc Interv Radiol 2006; 17:1251–1278.

ACKNOWLEDGEMENTS: The present work was supported by the scientific research project CEEX 100/2006 (MATNANTECH) of the Romanian Excellence Research Program.

European Cells and Materials Vol. 13. Suppl. 3, 2007 (page 42) ISSN 1473-2262

Three Dimensional Micro-Structure of Scaffolds for Tissue Replacement

S.Gürel[1], A.Braccini[2], I.Martin[2], F.Beckmann[3], and B.Müller[1]

[1] *Biomaterials Science Center, University of Basel, Switzerland*

[2] *Departments of Surgery and of Research, University Hospital Basel, Switzerland*

[3] *GKSS-Research Center, Geesthacht, Germany*

INTRODUCTION: Bone tissue engineering aims to fulfil the need to provide bony tissue for skeletal use. In spite of the fact that the allogenic bone or autogenous grafts have been used for decades, disadvantages like failure of complete resorption of autogenous bone raises the demand to have alternative approaches, which puts bone tissue engineering into play. Usage of three-dimensional (3D) porous ceramic scaffolds in bone tissue engineering manifests itself as a promising methodology for treatment of a wide range of clinical situations, challenging to replace former methods like allografts, synthetic materials etc. Scaffold characteristics such as porosity, interconnectivity and especially morphology on the micrometer scale are crucial for optimizing cell attachment and the related osteointegration.

METHODS: In this study, the micro-architecture of hydroxyapatite scaffolds with the diameter of 8 mm and the height of 4 mm is uncovered. The scaffolds (Engipore; Fin-Ceramica Faenza, Faenza, Italy[1]) have a total porosity of 83% ± 3%. In order to determine the interconnectivity, the scaffold was embedded into paraffin.

Synchrotron radiation-based micro computed tomography (SRμCT) in absorption contrast mode[2] from the beamline W 2 at HASYLAB/DESY, Hamburg, Germany with the photon energy of 30 kV provided the morphology of the opaque constructs with a pixel length of 4.3 μm and a spatial resolution of 7.4 μm.[3]

RESULTS: Figure 1 shows the morphology of the porous scaffold by means of two virtual slices perpendicular to each another. The pores do have a spherical shape. Many of them seem to be connected. In order to determine the degree of interconnectivity the pores were filled with paraffin, which is visualized in Fig. 1 on the right by the red color. Paraffin was segmented by intensity-based thresholding possible as the consequence of the lower X-ray absorption with respect to the scaffold material. The paraffin clearly penetrated through all pores. Some pores, however, are incompletely filled with the paraffin. They are just covered at their periphery by a thin film with a thickness of at least 40 μm.

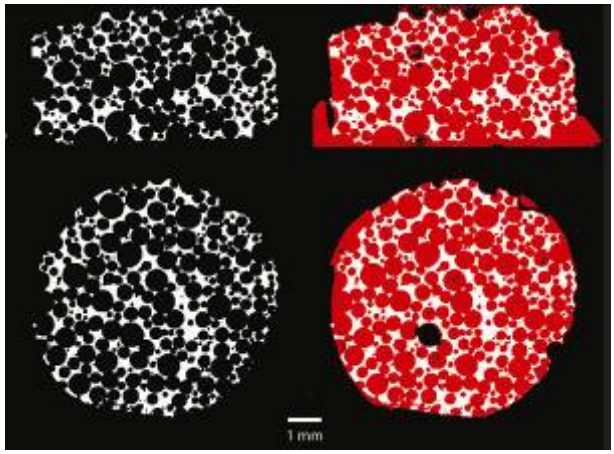

Fig. 1: The frontal and axial slices virtually cut from the SRμCT data demonstrate the spherical shape of the pores. The same slices are reproduced together with the penetrated paraffin (red colored) to verify the interconnectivity of the pore network.

DISCUSSION & CONCLUSIONS: 3D micro architecture of porous ceramic scaffolds is made visible using SRμCT. The visualization of penetrated paraffin revealed that the pores are well interconnected. The channels between the spherically shaped pores, however, are quite thin and are, therefore, incompletely filled.

The data allows further quantification based on sophisticated computer vision tools including component labelling, growing region and dilatation procedures.

REFERENCES: [1]http://www.finceramica.it
[2]F. Beckmann et al. (2006) *New Developments for synchrotron-radiation-based microtomography at DESY*, Proc SPIE **6318**:631810. [3]B. Müller et al. (2002) *Non-destructive three-dimensional evaluation of biocompatible materials by microtomography using synchrotron radiation*, Proc SPIE **4503**:178-188.

ACKNOWLEDGEMENTS: This project is supported by HASYLAB at DESY, Hamburg, Germany (proposal I-05-028).

European Cells and Materials Vol. 13. Suppl. 3, 2007 (page 43) ISSN 1473-2262

Investigation and Development of the Osseous Part of BoneWelding® Hybrid Implants

M.Röllinghoff[1], S.Saladin[1], J.Mayer[2], R.Müller[1]

[1] *ETH Zurich, Department of Mechanical & Process Engineering, Switzerland.*
[2] *WW Technology AG, Schlieren, Switzerland*

INTRODUCTION: To enhance the stability of the bone-implant interface, a new process, the BoneWelding® Technology, has been developed during the recent years by WoodWelding AG offering new alternatives in the treatment of fractures and other degenerative disorders of the muskuloskeletal system[1,2]. The BoneWelding® process employs ultrasonic energy to liquefy a thermoplastic interface between orthopaedic implants and the host bone. The BoneWelding® process is compatible with many thermoplastics, including current resorbable orthopaedic polymers. Significant potential is seen in so called hybrid concepts, wherein the polymer is applied on the load bearing implant as a complete coating. This concept allows the combination of the load transfer characteristics of the polymer-bone interface with the high mechanical properties of metallic or ceramic core material. The aim of this project was to investigate and develop the osseous part of such a novel hybrid implant with titanium core and resorbable polymer coating (see Figure 1).

METHODS: Preliminary design and feasibility studies were performed, using aluminium and polycarbonate as substitute material for titanium and the resorbable polymer (PLDLLA 70/30). A specially designed bone model for normal and osteoporotic bone, consisting of aluminium foams, epoxy plates as cortical bone model and bone marrow substitute was used for evaluating the implant designs before implanting the actual titanium-resomer-hybrids into bone (bovine proximal tibiae). Thermal analysis, along with pullout and bending tests were performed to evaluate the final implant performance and to compare the found design to commercially available Schanz- and Pedicle screws. Furthermore, different hybrid designs, as well as classic pedicle screws, were evaluated in a FEM study.

RESULTS: It could be shown that a homogenous infiltration of the polymer along the implant can be achieved and that infiltration depth can be controlled by the thickness of the polymer coating. In respect to the density of each bone sample, the hybrid implant showed a good performance in comparison with Schanz- and Pedicle screws. In osteoporotic bone model, the hybrid implant showed a significant higher performance due to the strong microinfiltration interphase between the polymer and the trabeculae (see Figure 2).

Fig. 1: Hybrid implant with titanium core and PLDLLA coating

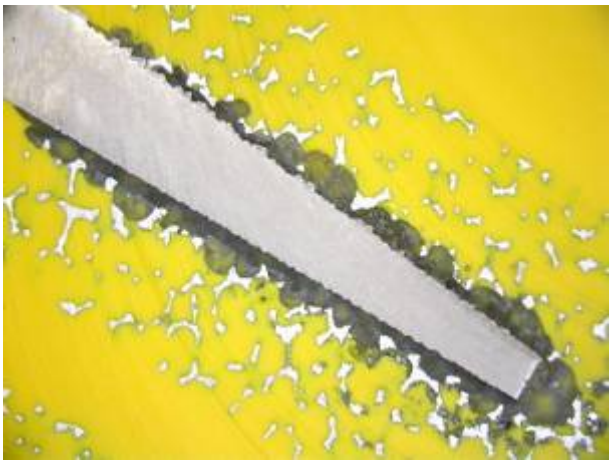

Fig. 2: Hybrid implant inserted into low densitiy aluminium foam (substitute material for osteoporotic bone)

DISCUSSION & CONCLUSIONS: The obtained results show a very promising potential of the developed hybrid implants, especially when applied in osteoporotic bone.

REFERENCES: [1] S.J. Ferguson, et al (2006) *Enhancing the Mechanical Integrity of the Implant-Bone Interface With BoneWelding® Technology: Determination of Quasi-Static Interfacial Strength and Fatigue Resistance*, J Biomed Mater Res Part B: Appl Biomater 77B: 13-20. [2] D.C. Meyer, et al (2005) *Ultrasonically Implanted Suture Anchores Are Stable in Osteoporotic Bone*, Clin. Ortho. Rel.Res 442m 143.148 .

ACKNOWLEDGEMENTS: The authors like to thank the WW Technology AG in Schlieren for providing essential support to their work.

Electrospinning of Polyesters

S.Schweizer[1], A. Taubert[2]

[1]*Departement of Chemistry, University of Basel, Klingelbergstrasse 80, 4056 Basel, Switzerland*
[2]*Institute of Chemistry, University of Potsdam, Karl-Liebknecht-Str. 24-25, Building 26, Room 2.64, 14476 Golm, Germany*

INTRODUCTION: Electrospinning is a unique procedure using electrostatic forces to make fine fibers with diameters in the range of nanometers to a few microns from solutions or melts. These fibers may act as highly porous scaffolds for tissue engineering, among others. So far, we have spun some poly(ε-caprolactone) (PCL)- fibers by variation of several parameters using a self constructed apparatus. Subsequently we want to spin PCL and other polyesters as scaffolds for Calcium Phosphate mineralization.

METHODS: The apparatus used for electro-spinning consists of a high voltage electric source with positive or negative polarity, a syringe pump with capillaries or tubes to carry the solution from the syringe to the capillary, and a conducting collector like aluminium (Figure 1).The final fibrous structure can be tailored by altering the concentration of the polymer solution, the molecular weight and molecular-weight distribution, the applied voltage, the solution flow rate and the distance between the capillary and collector. The effects of the preparation conditions on the fiber diameter were observed by optical microscopy and scanning electron microscopy (SEM).

Fig. 1: Configuration of our Electrospinning apparatus.

RESULTS: Most effective parameter variations are polymer concentration and flow rates of the polymer solutions. If the flow rate is low, the capillary may plug. On the other hand, no continuous jet will form when the flow rate is too high. Spinning with different polymer concentrations leads to different fiber diameters, nonfibrous structure, and bead-rich scaffolds.

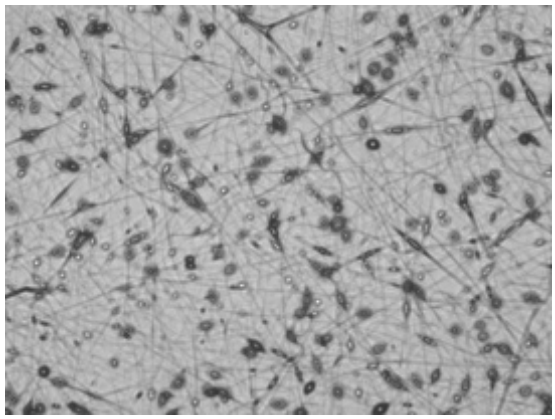

Fig. 2: Optical Microscope Image (20x) from 7 % wt PVL (80kDa) in Dichloromethane at 22.5 kV with 0.8 ml/h solution flow.